

**COMPARISON OF NEUTRONIC SAFETY PARAMETERS OF
SOME COMMERCIAL PWRS UNDER CONSIDERATION FOR
GHANA'S FIRST NUCLEAR POWER PLANT**

By

Atsu, Mensah Kwaku Prince

A Thesis submitted to

The Graduate School of Nuclear and Allied Sciences
University of Ghana, Legon

In partial fulfilment of the requirements for the

Degree of

MASTER OF PHILOSOPHY IN NUCLEAR ENGINEERING

Department of Nuclear Engineering
College of Basic and Applied Sciences

July, 2017

DECLARATION

I hereby declare that, this thesis is the undertaken of PRINCE MENSAH KWAKU ATSU under the supervision of Dr. ROBERT BRIGHT MAWUKO SOGBADJI and Dr. REX GYEABOUR ABREFAH both of the School of Nuclear and Allied Sciences (SNAS), University of Ghana (UG).



.....

PRINCE MENSAH KWAKU ATSU

DATE:

.....

DR. ROBERT B. M. SOGBADJI
(Principal Supervisor)

.....

DR. REX G. ABREFAH
(Co-Supervisor)

DATE:

DATE:

DEDICATION

This work is dedicated to my grandparents, Mensah Kofi Atsu, Atado Kofi Atsu, the late Lisashie Kumi and the late Happy Lumorshie Adukpo.



ACKNOWLEDGEMENTS

Firstly, I am most grateful to the Almighty God who endowed me with the strength to undertake this research. He has indeed brought me to an expected end and all honour, praise and glory is due Him.

I wish to express my sincere gratitude to all my lecturers, especially my supervisors Dr. Robert Bright Mawuko Sogbadji and Dr. Rex Gyeabour Abrefah of the Department of Nuclear Engineering for their expert guidance, advice and encouragement. I say a big thank you.

My special thanks also goes to my parents; Dr. Daniel Workman Atsu, WOII Rt. Alex Atsu and Mrs. Rejoice Wemega for relentlessly funding my education all these years.

I am highly indebted to my best friend Evangeline Enyonam Gakpleadzi for her support and encouragement when times were tough- Enyo, you are really special.

My heartfelt appreciation goes to my family, especially Gifty Wemega for the moral support and encouragement.

Lastly, my profound gratitude goes to my friends and course mates who have in diverse ways helped me in the fulfilment and success of this study. Martin Dugble, Emmanuel Nyogbe, Benard Osei-Tweretwie and Victor Caesar Manowogbor, I say thank you.

TABLE OF CONTENTS

DECLARATION	ii
DEDICATION.....	iii
ACKNOWLEDGEMENTS.....	iv
TABLE OF CONTENTS.....	v
LIST OF TABLES.....	viii
LIST OF FIGURES	ix
LIST OF ABBREVIATIONS.....	xi
NOMENCLATURE	xii
ABSTRACT.....	xiii
CHAPTER ONE.....	1
1.0. INTRODUCTION	1
1.1. General Introduction	1
1.2. Research Problem	6
1.3. Research Objectives.....	7
1.4. Justification for the Study.....	7
1.5. Scope and Limitation of Study	8
1.6. Organization of Research.....	8
CHAPTER TWO	10
2.0 LITERATURE REVIEW	10
2.1 General.....	10
2.2 Overview of the Pressurized Water Reactor designs	11
2.2.1 European Power Reactors (EPR).....	13
2.2.2 EPR Design Overview	13
2.2.3 Vodo-Vodyanoi Energetichesky Reactors (VVER-1000)	17
2.2.4 Design Overview of the VVER-1000	18
2.2.5 High Pressure Reactor (HPR1000)	21
2.2.6 Design Overview of the HPR-1000	22
2.3 Overview of Neutronic Safety Parameters of Nuclear Reactors.....	24
2.3.1 Void Coefficient.....	27
2.3.2 Temperature Reactivity Coefficient.....	29
2.4 Concluding Remarks.....	32

CHAPTER THREE	33
3.0 THEORITICAL ANALYSIS	33
3.1 Introduction.....	33
3.2 Nuclear Reactor Theory	33
3.3 Neutron Transport Theory	34
3.4 Methods Used to Solve or Simulate Neutron Transport	36
3.4.1 Deterministic Methods.....	36
3.4.2 Stochastic Methods	37
3.5 Monte Carlo Technique	38
3.5.1 MCNP Tallies	39
3.5.2 Neutron Flux and Power Distribution.....	40
3.5.3 Cross-Section Data.....	41
3.5.4 Determination of Fission Cross Section.....	42
3.5.5 Treatment of Thermal Neutrons.....	43
3.5.6 Criticality Calculations	43
3.5.7 Convergence	45
3.5.8 Theory of Convergence of k_{eff} and Fission Source Distribution	46
3.6 Estimation of Monte Carlo Precision.....	47
3.6.1 Estimated Mean	48
3.6.2 Relative Error.....	49
3.6.3 Variance of Variance	49
3.6.4 History Score Probability Density	50
CHAPTER FOUR.....	52
4.0 METHODOLOGY	52
4.1 Introduction.....	52
4.2 MCNP5	53
4.2.1 MCNP5 Input File Description.....	53
I. Section 1/Title card.....	54
II. Section1/Cell cards.....	54
III. Section2/Surface cards.....	55
IV. Section3/Data cards	55
4.3 MCNP5 Model of the Reactors.....	56
4.3.1 Model of the HPR and EPR	58
4.3.2 Model of the VVER.....	60

CHAPTER FIVE	62
5.0 RESULTS AND DISCUSSION	62
5.1 Introduction.....	62
5.2 Moderator Void Reactivity	62
5.2.1 Moderator Void Coefficient of Reactivity	66
5.2.2 Neutron Spectra of Different Reactors with Same Void Content	68
5.3 Moderator Temperature Reactivity.....	71
5.4 Doppler Effect of U-238 on Reactivity	73
CHAPTER SIX.....	78
6.0 Conclusion and Recommendation	78
6.1 Conclusion and Recommendations.....	78
7.0 References.....	80



LIST OF TABLES

Table 4.1: Sections of MCNP Input file	54
Table 4.2 Fuel Assemblies Design Specifications	57
Table 5.1 Moderator Void Coefficient of Reactivity at Different Void Fraction	67



LIST OF FIGURES

Figure 1.1 Schematic diagram of a Pressurized Water Reactor.....	6
Figure 2.1 Simplified EPR plant layout	14
Figure 2.2 EPR Reactor Pressure Vessel	15
Figure 2.3 Simplified VVER-1000 plant layout	19
Figure 2.4 TVSA General view	21
Figure 2.5 HPR plant layout	23
Figure 2.6 Plot of Reactivity against Moderator Void Fraction for a typical French EPR	28
Figure 2.7 Change in Reactivity against Moderator Temperature for a typical French EPR	30
Figure 4.1 MCNP5 Plot of Transverse Section of EPR and HPR Fuel Pins	59
Figure 4.2 MCNP5 Plot of Longitudinal Section of the EPR and HPR Fuel Pins	59
Figure 4.3 MCNP5 Plot of Transverse Section EPR and HPR Fuel Assemblies	60
Figure 4.4 MCNP5 Plot of Transverse Section VVER Fuel Assembly	61
Figure 5.1 Moderator Void for the Three Assemblies.....	63
Figure 5.2 Neutron Spectra of different percentage of Loss of Coolant for the EPR Assembly.....	64
Figure 5.3 Neutron Spectra of different percentage of Loss of Coolant for the HPR Assembly.....	65
Figure 5.4 Neutron Spectra of different percentage of Loss of Coolant for the VVER Assembly.....	65
Figure 5.5 Neutron Spectra for EPR, HPR and VVER at Normal Operating Void	68
Figure 5.6 Neutron Spectra of EPR, HPR and VVER at 50% Void.....	69
Figure 5.7 Neutron Spectra of EPR, HPR and VVER at almost 100% Void.....	70
Figure 5.8 Moderator Temperature Coefficient of the Three Reactor Assemblies	72
Figure 5.9 Doppler Broadening Effect in EPR Assembly	74

Figure 5.10 Doppler Broadening Effect in HPR Assembly..... 74

Figure 5.11 Doppler Broadening Effect in VVER Assembly..... 75

Figure 5.12 Doppler Effect of the Three Reactors at 50% Increase in Temperature... 76

Figure 5.13 Doppler Effect of the Three Reactors at 50% Increase in Temperature... 77



LIST OF ABBREVIATIONS

Abbreviation	Definition
EPR	European Pressurized Reactor
FSAR	Final Safety Analysis Report
Gd ₂ O ₃	Gadolinium Oxide
GWe	Giga watt electric
GWt	Giga watt thermal
HPR	High Temperature Pressurized Reactor
LWR	Light Water Reactor
MCNP5/MCNP	Monte-Carlo N-Particle
MeV	Mega electron volts
MTC	Moderator Temperature Coefficient
MW	Mega watt
MWt	Megawatt thermal
PWR	Pressurized Water Reactor
RCCA	Rod control cluster assembly
RCP	Reactor Coolant Pump
RPV	Reactor Pressure Vessel
RTC	Reactivity Temperature Coefficient
SAR	Safety Analysis Report
UO ₂	Uranium Oxide
VVER	Vodo-Vodyanoi Energetichesky Reactor

NOMENCLATURE

k_{∞}	Infinite multiplication factor
k_{eff}	Effective multiplication factor
η	Reproduction factor
f	Fuel utilization factor
ε	Fast fission factor
ρ	Resonance escape probability
P_{NL}	Non leakage probability
W_t	Particle weight
T_l	Track length (cm)
V	Cell volume (cm ³)
ϕ	Neutron flux (neutrons/cm ² -s)
σ	Microscopic cross-section (barns)
Σ	Macroscopic cross-section
S	Neutron Source
\vec{r}	Directional vector
E	Energy (eV)
t	Time (s)



ABSTRACT

Ghana is presently exploring the option of including nuclear power plant technologies into the country's electricity generation mix. As part of technology assessment, investigative studies of some neutronic safety parameters of the proposed nuclear reactor technologies are carried out and compared in this study.

This study focuses on neutronic safety analysis of reactor technologies under consideration, these are; the European Pressurized Reactor (EPR), High Temperature Pressurized Reactor (HPR) and the Vodo-Vodyanoi Energetichesky Reactor (VVER). The input model of all three reactors were successfully developed and simulated. Analysis of the Reactivity Temperature Coefficients, Moderator Void Coefficient, Criticality and Neutron Behaviour at various operating conditions was carried out using the Monte Carlo N-Particle (MCNP5) code and the results referenced with values in literature.

The nuclear power reactor technologies under study showed good safety inherent features. All three reactors gave negative coefficients for both increasing moderator temperature and moderator void fraction which was consistent with safety inherent features. The VVER assembly had the largest absolute value for the coefficients of reactivity from 0% to 80% void fraction as compared to the other technologies under study. Even though all technologies showed Doppler broadening with increasing temperature, the EPR had the highest absorption cross section, showing a higher safety margin.

CHAPTER ONE

1.0. INTRODUCTION

1.1. General Introduction

In today's world, energy has become a decisive lifeblood of the global economy. To maintain and improve the living conditions of the growing population of the world, a dependable, consistent and reasonably priced energy is needed. Industries, factories and cities rely on heat, light and power to run and provide jobs, homes, goods and services for people to enjoy the amenities and make life more satisfactory and pleasant. The growing population of the world demands an increase in energy consumption, as such, energy demands keep rising, most especially in the developing world (Yergin & Gross, 2012).

Energy use and development vary widely across the African continent. The World Bank has declared 25 of the nations on the continent to be in energy crisis. Energy development has not kept pace with the rising demand in developing regions, placing a strain on the continent's existing resources over the first decade of the new century. The GDP for over half of the countries in sub Saharan Africa rose by 4.5% annually between 2001 and 2005, while energy generation capacity grew at a rate of 1.2% over the same period (World Bank, 2013).

In Ghana, electricity generation has seen several phases of developments: first was the industrial mine and factory owned diesel generators and standalone electricity supply system through to hydroelectric generation from the Akosombo dam and now to the complementary gas and crude powered thermal power plants. Over the years, efforts to add to the energy generation in the country has failed to match the growing demand in

consumption. This has led to the embarrassing rationing of power in the country. This seemingly perpetual power crisis poses serious developmental challenge to the state. The economic transformation and growth that the country aspire is seriously being thwarted by the soar in severity of the power crisis. The distressful load shedding, the impediment on industrial production, the loss of income and revenue the growing unemployment and job losses and the constant interruptions in social activities is a clear indication of what has now become a never-ending frustration on Ghana's development agenda (Eshun & Amoako-Tuffour, 2016). For rapid and optimized industrialization, it is crucial that energy generation meets the demand, this will give the Ghanaian economy the impetus to develop and grow. Currently in Ghana, electric power is generated from hydro, fossil and various renewable sources such as wind and solar. Adoption of nuclear energy into the country's energy mix will help in closing the current electricity supply deficit and eliminating the difficulties being faced by both industrial and domestic users and stabilize the prices of utilities. The increasing demand for electricity power supply as a result of population increases and industrial expansions, calls for accelerated measures to venture into nuclear power to ensure sustainable economic growth (CEPA, Center for Policy Analysis, 2007).

Throughout the world, we need every energy source we can get - including nuclear. A number of advantages warrant the use of nuclear energy as one of the many methods of meeting the high demand of energy. Its appeal lies in immeasurable quantities such as its "cleanliness" (environmentally friendly), cheap transportation, and high fuel energy density (1 g of Uranium can produce approximately 90,000x more energy as 1g of coal). The technology for nuclear energy generation is also well- developed, as opposed to photovoltaics for example, the technology for which is still under development as energy efficiencies are increased (Singh, 2015).

Nuclear reactors are used to harness the energy released from nuclear fission reactions to generate heat which most often is used to turn turbines to generate electricity. A nuclear reactor is an assembly of appropriate materials carefully arranged to initiate, sustain and control fission chain reaction. Nuclear reactors can be differentiated either by its use or by the design features. A nuclear reactor could be used as a research reactor which have relatively a smaller size or as a power reactor which is quite large. Mainly, research reactors are operated to produce enough neutron flux for neutron activation analysis. Also, the neutrons from the research reactor could be used to produce radiopharmaceuticals for medical diagnoses and therapy, material testing and for research purposes as the name suggests. These reactors could be operated in countries where there is no nuclear power. Ghana currently operates a research reactor located at the reactor centre of the Ghana Atomic Energy Commission. Power reactors on the other hand makes the major component of a nuclear power plant primed for the production of electricity. Residual heat from power reactors could be used for desalination of sea water and in small units, can be used to propel ships. Currently, over 30 countries operate nuclear power plants. (Larmash R. J., 2001). This study is restricted to power reactors.

Nuclear power reactors differ in many ways although they are all designed to produce energy from the fission of heavy nuclei to be converted to mechanical energy then ultimately to into electrical energy. Heavy atoms such as thorium, uranium and plutonium are utilized as fuel in these reactors. The energy from fission is as a result of the bond energy released in the form of kinetic energies carried by the fission products and neutrons born from fission. The kinetic energy is transformed to heat energy in the fuel and moderator material which decelerate the fission products and neutron (Sogbadji, 2012). The heat generated during the fission is transferred to a fluid acting

as a coolant. In the case of gas cooled reactors, the heated gas is fed directly into a turbine driving alternator. For liquid cooled reactors, heat from the coolant is used to generate steam in a steam generator which is then fed into the turbine. The heat energy is not fully transformed to another form according to the laws of nature. The residual heat is discharged directly into the environment through water bodies or indirectly through cooling towers. The release of residual heat is not restricted to nuclear plants but is a common practice to all types of thermal plants (Sogbadji, 2012).

Currently, a total of 447 nuclear power are plants operating worldwide today with 391,067 MWe installed capacity. Out of this, about 350 are light water equipped (IAEA, 2017). Thanks to its high safety standards and operational reliability. Light water reactor technology has for many years enjoyed a degree of maturity that makes it one of the leading power plant concepts for the power generation industry. Availability ratings of 90% and more, equivalent to over 8000 operating hours per annum, have become the norm for many plants (Brettschuh & Schneider, 2002). Codes and standards governing the licensing procedure for light water reactor construction and operation as well as operational monitoring are also well established. It was therefore clearly in the interest of plant vendors, as well as the utilities, to further develop these plant designs on the basis of the excellent operating experience gained in the past (Schneider, 2002).

Ghana has made known of its intention to generate electricity using nuclear energy in the near future and plans are far advance in its implementation. It is therefore imperative that neutronic analyses are performed on the available commercial nuclear power designs and technologies to assess the safety of the nuclear technologies under consideration based on their neutronics and the appropriate recommendations made to the institutions responsible for the choice of the design and technology. It must be noted

that the choice of technology is not solely dependent on the neutronic parameters but also depends on other equally important factors.

For the purpose of this study, the neutronic parameters of three commercial pressurized water reactors (PWR) shall be compared; the reactors are the Chinese HPR-1000, Russian VVER-1000 and the French EPR-1000. This work will be focused on the neutron flux spectrum at different conditions for each reactor, loss of coolant (void coefficient), temperature coefficient and the multiplication factor (k_{∞}) at different stages and conditions of these reactors. Neutron behaviour and distribution in the reactor core is given by the neutron spectrum. The neutron spectrum is a function characterized by the energy dependence of neutron flux $\phi(r,E,t)$ and it is affected by fuel enrichment, moderator density, void fraction, burnup, and moderator and fuel temperature (Okumura, Oka, & Ishiwatari, 2014). Neutron multiplication is very sensitive to temperature and density changes of the materials. Water density changes have a much greater effect on reactivity.

Void formation or changes in moderator density has a prevailing effect on reactivity in water moderated reactors. Loss of coolant in light water reactors is associated with a decrease in moderator density which results in increase in resonance. In water moderated reactors, about 80% of the moderation occurs inside the moderator of the reactors (Khan, Villa, & Bock, 2011). Therefore void effects on core reactivity of the three reactors will be studied in this work. One important quantity in determining the operating characteristics and safety of nuclear reactors is the temperature coefficient of reactivity. The isothermal temperature coefficient in Light Water Reactors (LWR) varies considerably with the design, the moderator temperature and the boron concentration in the moderator (Edenius, 1976). Below is a schematic diagram of a

pressurized water reactor and how it produces electricity from the heat generated in by the fission reaction.

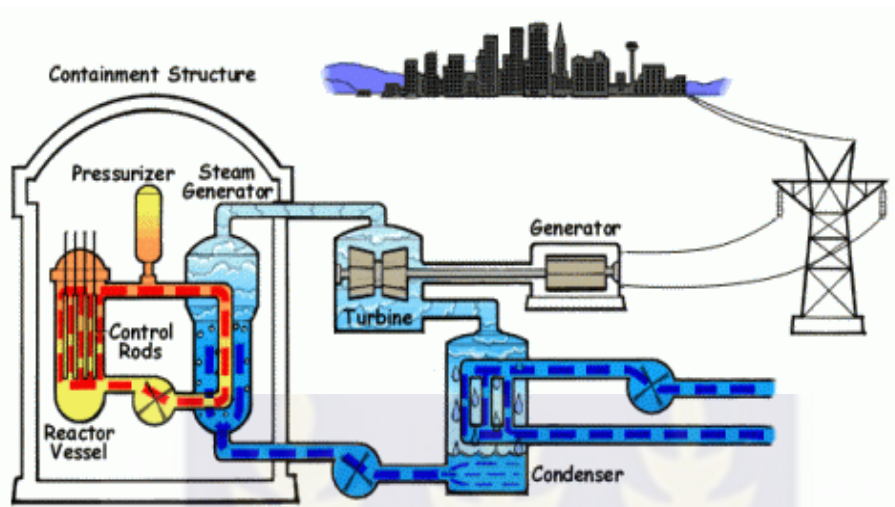


Figure 1.1 Schematic diagram of a Pressurized Water Reactor

1.2. Research Problem

Nuclear power reactors vary based on their technology, design and the material composition of the various components of the reactor. This inevitably has notable effect on the neutronics which is the main safety parameter for nuclear reactors.

With Ghana's decision to go nuclear, the state will have to settle on one of the available nuclear technology. Ghana will have to evaluate and analyse all the existing candidate technologies to ascertain which technology has the best neutronic safety and inherent passive safety mechanism for a new-comer country like Ghana.

1.3. Research Objectives

The objectives of this work are to;

1. Determine the neutron spectra of the Chinese HPR-1000, Russian VVER-1000 and the French EPR-1000 reactors using MCNP at various moderator voids to mitigate LOCA
2. Determine the infinite multiplication factors of Chinese HPR-1000, Russian VVER-1000 and the French EPR-1000 reactors using MCNP at various operation conditions.
3. Determine the moderator temperature coefficients and void coefficient of the various reactors in an accident scenario and their effect on reactivity using MCNP.
4. Make recommendations on choice of reactor technology to the Ghana Nuclear Power Programme based on the results obtained from this work.

1.4. Justification for the Study

Ghana's position for nuclear power has made the studies on the efficiency and safety of the available nuclear power technologies a necessity. Neutronic safety parameter measurements in the nuclear reactors under consideration is the most important factor with respect to safety and efficient operation. The reactor design process is significantly affected by the design and distribution of fuel assemblies inside the core. Therefore, safety in the design of a reactor greatly depends on the accuracy of neutronics calculations in fuel assembly design.

Temperature and moderator coefficients are required to enable a reactivity assessment to be made and to deduce the magnitude of the reactivity change to be expected with

the temperature and moderator variation. This effect may alter the complete mode of operation of the reactor.

1.5. Scope and Limitation of Study

For the purposes of analysis of nuclear technologies, both neutronic and thermal hydraulics as well as radiological safety assessments are very important. However, this study is concentrated on the neutronic calculations in the three pressurized water reactors mentioned earlier. Parameters such as the infinite multiplication factor (k_{∞}), moderator temperature coefficient, void coefficient and the neutron flux spectrum will be considered.

The MCNP code will be employed as a computational tool to help obtain the result.

1.6. Organization of Research

The entire study shall be organised in five chapters. The first chapter will cover a brief introduction to the study, the research problem statement, justification of the study, research objectives, scope and limitations of the research as well as the organization of the research.

The second chapter will discuss literatures that are relevant to the study. To follow that will be the chapter three which will focus on the methodology and fundamental equations employed in the design and simulation process.

In the chapter four, the data presentation and analysis of results in the form of tables and graphs will be presented. The research will be concluded with the chapter five

which covers a summary of the findings, conclusions and if there is the need for further studies, appropriate recommendations shall be made.

Various studies carried out on LWRs shall be reviewed in the next chapter, particularly, studies carried out on the VVER, HPR and EPR in the areas of their neutron flux spectrum, infinite multiplication factor and reactivity coefficients.



CHAPTER TWO

2.0 LITERATURE REVIEW

2.1 General

Public scepticism and fear for nuclear has grown following the Fukushima Daiichi nuclear accident. Despite this, demand for nuclear power continues to grow steadily at a slower rate two years on (IAEA, 2013). Currently, there are about 447 nuclear power plants operating worldwide and about 68 being constructed, giving a global nuclear power generation capacity reaching 391.1GWe. Of the total of 438 operational nuclear power plants, about 347 are equipped with light water reactors (LWRs), which are the pressurized water reactors (PWRs) and the boiling water reactors (BWRs). Both reactor types contributing an availability ratings of 90% and more, equivalent to over 800 operating hours per annum (IAEA, 2017).

A number of countries including Ghana continue to push for the addition of nuclear power into their energy mix despite the Fukushima Daiichi nuclear accident, due to the persistent need for cheap, sustainable and reliable power. Nuclear power programs today represent an increasingly competitive, safe and reliable source of energy that responds to stringent demands for environmental protection (Ghana News Agency, 2014).

Safety analysis of reactor systems continues to be crucial in reassuring the public of the safety and reliability of nuclear power plants. Safety analysis is also crucial in aiding countries to make decisions on the type of reactor systems to build and also to incorporate the lessons learnt from nuclear accidents into safety analysis for added safety assurance (Motwendi, 2014).

2.2 Overview of the Pressurized Water Reactor designs

Currently, the most common type of commercial nuclear power reactors is the pressurized water reactor, often known by its abbreviation PWR. The first PWR reactors were designed for military ship propulsion by the Westinghouse Bettis Atomic Power Laboratory and then commercialized by the Westinghouse Nuclear Power Division. The 60MWe Shippingport located in Pittsburgh, Pennsylvania in the United States was the first commercial PWR.

The Russian version of the commercial pressurized water reactor was developed from nuclear submarine and ice breaker experience. The Russian PWR is known as VVER which is an abbreviation for Vodo-Vodyanoi Energetichesky Reactor which translates as “water-cooled water-moderated reactor”. Hence, operating PWRs are generally classified into U.S/Europe type and Russia type (VVER). Nuclear power plants from Russia differ in many ways from Western nuclear power plants, a typical example is the horizontal steam generators in the VVERs while western plants have two, three or four large vertical steam generators.

The PWR consists of two main systems; a primary (reactor) system and a secondary (steam) system. This is to confine the radioactive materials to the reactor system. In the primary loop, heat is generated from the controlled fission reaction into the coolant at a pressure of about 15.5 MPa so that it circulates within the primary loop at a high temperature of 325 °C without boiling. At the steam generator, heat is removed from the coolant (primary loop) into the secondary loop where steam is generated. The coolant is then pumped back to repeat the cycle. A pressurizer is connected to keep the pressure above saturation pressure to prevent bulk boiling in the reactor system. In the secondary loop, the steam produced in the steam generator is pumped to a turbine which

drives a generator to produce electrical energy. The steam is then condensed and pumped back into the steam generator to repeat the cycle.

The reactor vessel houses the core barrel, the heat-generating core, coolant circulating channels and associated supports and controls. The PWR has a cylindrical shaped reactor vessel with hemispherical heads at the top and bottom. The upper head is removable to allow for refuelling of the reactor. The coolant loop of the reactor system has an inlet nozzle at the “cold leg” and an outlet nozzle at the “hot leg”. The fuel is surrounded by the core barrel fitted inside the reactor vessel. It creates an annular channel to enhance coolant flow and also protects the vessel by attenuating some of the radiations emanating from the radioactive fuel. The fuel assembly sits on the lower core supporting plate at the bottom of the core barrel.

The reactor core consists of 150 to 200 fuel assemblies arranged in a square lattice. Typically, a PWR fuel assembly has between 200 and 300 fuel rods arranged in a 15 x 15 to 17 x 17 square array. Within the fuel assemblies are control rods which are incorporated into the assembly by control guide tubes which replace up to a third of the fuel rods. Other rods within the assemblies contain no fuel and are filled instead by instrumentations and burnable poisons such as boron to extend the core life. The fuel is made of UO_2 pellets with enrichment between 2.1 to 3.5% in U-235. These pellets are 0.813 cm in diameter and 1.53 cm in length. The pellets are pressed and enclosed in a Zircalloy-4 cladding tube with a wall thickness of about 0.064 cm. Zircalloy has a very good mechanical strength and more importantly, a low neutron absorption cross-section helping the neutron economy in the PWR.

Ordinary light water is utilized as both coolant and moderator in all PWR designs. The water enters the core at a temperature of about 257°C via the bottom. The water is

heated as it flows through the reactor core and exits the core at a temperature of about 315 °C. Like all other thermal reactors, the PWR requires that fast fission neutrons are thermalized in order to interact with the fissile U-235 in the nuclear fuel to sustain the nuclear chain reaction. This thermalization process is achieved through the multiple collision of the fast neutrons with light hydrogen atoms in the water moderator. Although heavy water has a much lower neutron absorption, light water is preferred in PWRs because of its strong moderation of neutrons.

2.2.1 European Power Reactors (EPR)

The EPR is a generation III+ evolutionary four-loop Pressurised Water Reactor (PWR) jointly developed by Framatome and Siemens through their subsidiary Nuclear Power International (NPI). It received technical support from the French utility Electricité de France (EDF) as well as from the German utilities who financed most of the development work (AREVA, 2012). The main components of the EPR design, loop configuration and primary system design are not different from operating PWR designs around the world. There are other EPR projects in progress in different countries around the world; “Finland (Olkiluoto), France (Flamanville), China (2 units Taishan) and some in the USA and UK” (AREVA, 2012).

2.2.2 EPR Design Overview

Like other PWRs, the four-loop pressurized water Reactor Cooling System (RCS), the reactor vessel containing the fuel assemblies, a pressurizer to maintain system pressure, Reactor Coolant Pump (RCP), steam generator and control and protection systems form the prominent components of the EPR. These components are shown in figure 2.1 below.

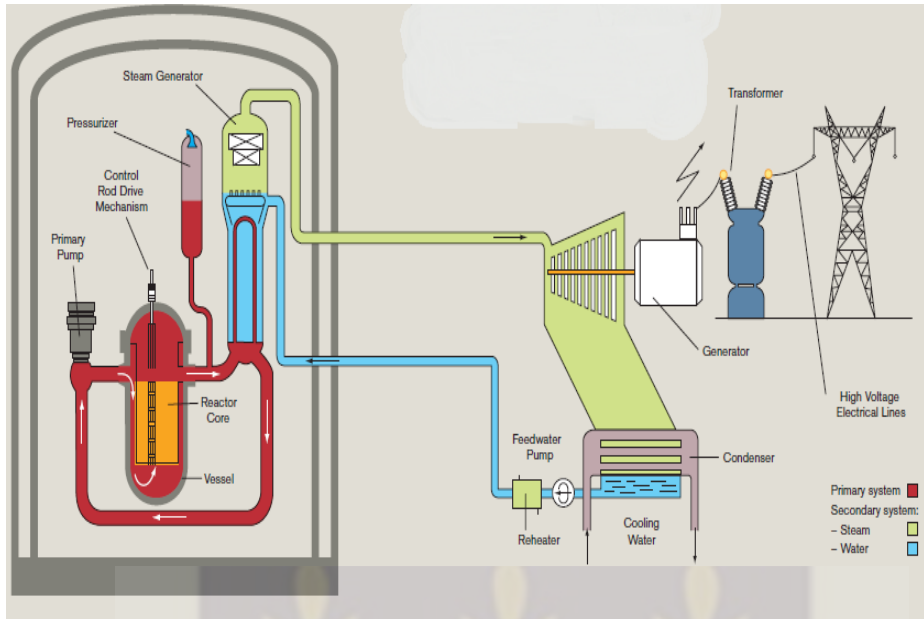


Figure 2.1 Simplified EPR plant layout

The EPR uses ordinary light water as both coolant and moderator to remove heat produced as a result of the fission process in the reactor core and decelerate fast fission neutrons born from the fission reaction in the core respectively. Slowing down the fast neutrons is important so that the neutrons are brought to thermal energies to be able to interact with the fissile atoms in the fuel to sustain the fission. The heat generated from fission in the core is carried by the primary coolant into the steam generator to be transferred to the secondary loop by the steam exchangers. The steam generated in the secondary loop is then pumped to drive the turbines to generate electrical energy (AREVA, 2012).

The EPR has new features like the redundant emergency core cooling trains, a shield and containment building and a core melt catcher for accidents. The volume required to contain the reactor core, heavy reflector, flow directing and supporting internals and the control rods is provided by the Reactor Pressure Vessel (RPV) with a diameter of

438.5 cm (AREVA, 2012). The reactor pressure vessel has thick walls made of low carbon alloy steel and internals made of NiCrFe alloy cladding to withstand the high operating pressures and increase resistance to corrosion. Within the RPV are four outlet and four inlet nozzles to provide connections to the four loops circulating the reactor coolant. Below is figure 2.2 showing the EPR RPV.

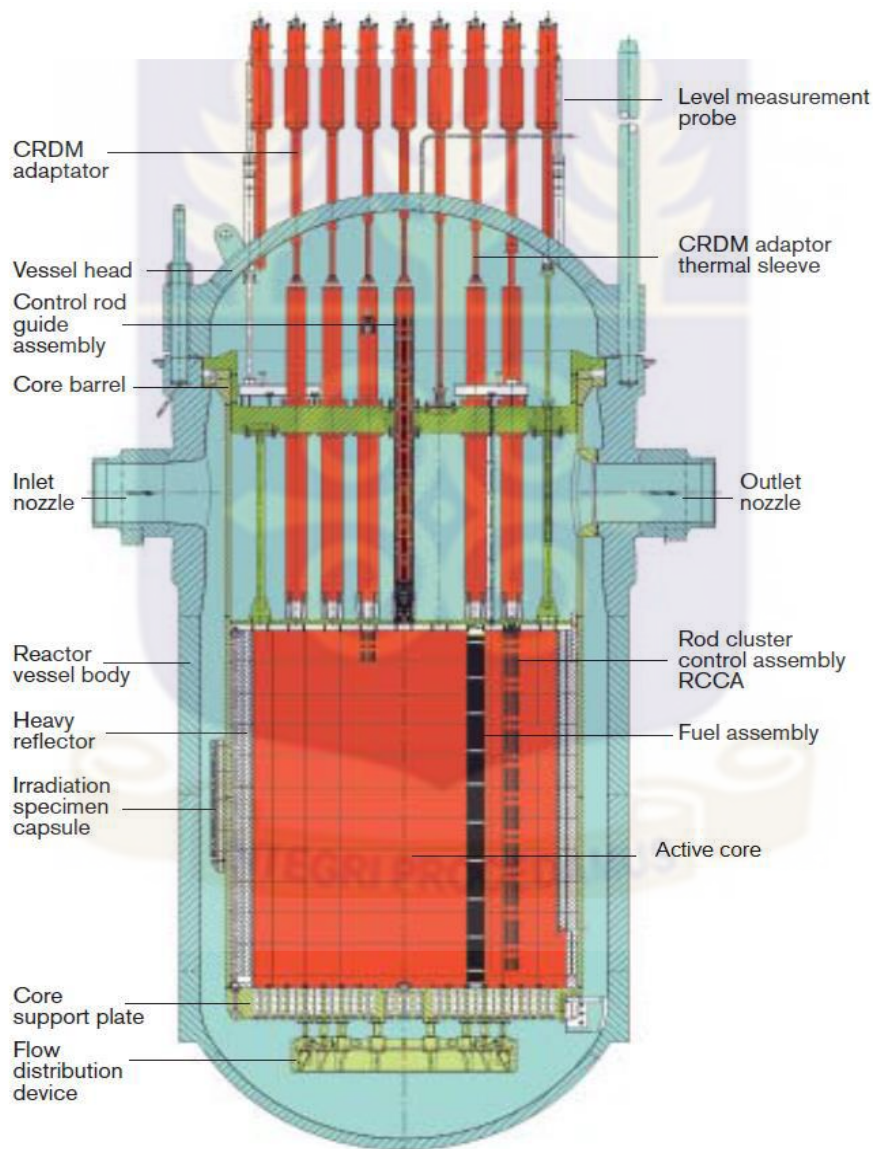


Figure 2.2 EPR Reactor Pressure Vessel

The reactor has a core with an active height of 420 cm and a rated thermal power of 4500 MWt. The core is designed to have a high thermal efficiency, low fuel cycle cost, and flexibility for extended fuel cycle lengths. The core cycle length is determined by the energy output required with the life time ranging from 12 to 24 months. The reactor core consists of 241 fuel assembly arrays. The fuel assemblies are arranged into a pattern to form a cylindrical shape. To prevent neutron leakage in the core, a heavy reflector which is a large steel structure of 10.2 to 20.3 cm width is used to surround the edge of the active core. This heavy reflector also flattens the core power distribution and reduces effects of the fast neutrons on the reactor pressure vessel (AREVA, 2012).

Core loading arrangement is not the usual expected loading, where the higher enriched fuel assemblies are located at the outer boundaries of the core. The initial core loading at beginning of life (BOL) consists of seven different fuel assembly neutronic designs with three rod types. Each fuel assembly's neutronic design for initial core loading contains a uniform distribution of gadolinium and uranium fuel elements. Fuel assemblies in the core are loaded such that the fuel assemblies with low enrichment are located at the outer boundary of the core to enhance fuel economy, while the ones with higher enrichment are distributed in the interior to establish a more favourable radial power distribution.

The fuel assembly has a 17 x 17 lattice design with 265 fuel rods, 23 guide tubes and one instrumentation. The fuel rod consists of cylindrical shaped uranium oxide (UO_2) pellets encapsulated in a zirconium alloy tube with plugs welded at each end. The zirconium alloy cladding offers resistance to corrosion associated with the high operating temperatures and high burn-up. The gap between the fuel meat and cladding offers an acceptable margin for failure due to pressure build up. The pellets are enriched

up to a value of 4.95 %wt. U-235 with tolerance of about 0.05%. The Rod Cluster Control Assembly (RCCA) each consists of 24 individual absorber rods fastened to a spider assembly. Silver (Ag) is the largest constituent of the absorber rod with 80 %wt. and Indium (In) and Cadmium (Cd) making up 15% and 5% respectively. The absorber material is sealed in a 316L stainless steel cladding tube to protect it against the coolant (Framatome ANP, Inc., 2005).

The RCCA are used for shut down and control reasons to compensate for the fast reactivity changes associated with:

- The required shutdown margin in hot zero power, all rods inserted condition with the most reactive rod stuck out.
- The reactivity compensation as resulting from power increase above hot zero power (power defect, Doppler and moderator reactivity changes).
- Unplanned boron concentration, xenon concentration or coolant temperature fluctuation.
- Reactivity ramp rates due to load changes.

Chemical absorbers are also used to control reactivity in the reactor. Typically, boron which is diluted in the moderator as boric acid is used as a chemical absorber in the EPR. The boron content is limited by the moderator coefficient.

2.2.3 Vodo-Vodyanoi Energeticheskoy Reactors (VVER-1000)

The VVER as it is mostly called is an abbreviation for Vodo-Vodyanoi Energeticheskoy Reactors which translates as ‘water water energy reactor’. The “water water” in the name depicts that ordinary water is for moderation and also as coolant in this reactor.

The number following the reactor type usually indicates the rated power of the unit (e.g. VVER-1000 designates a unit with 1000MW electrical power).

The VVER reactor itself was developed by ROSATOM subsidiary OKB Gidropress, while the nuclear power stations employing the VVER have been developed by the power plant design organizations within ROSATOM: Moscow Atomenergoproekt, Saint-Petersburg Atomenergoproekt (a branch of VNIPIET), and Nizhniy Novgorod Atomenergoproekt (ROSATOM, 2015). Many different versions of the VVER series reactor are in operation in many countries around the world especially in Eastern Europe (ROSATOM, 2011).

2.2.4 Design Overview of the VVER-1000

Similar to western PWRs, the VVER-1000 series reactor is a four-loop pressurised water reactor and has a containment similar to the western PWRs. The VVER-1000 has four loops with a steam generator in each loop. Like all other VVERs, the VVER-1000 use horizontal steam generators and two turbines. Figure 2.3 shows the layout of VVER-1000.



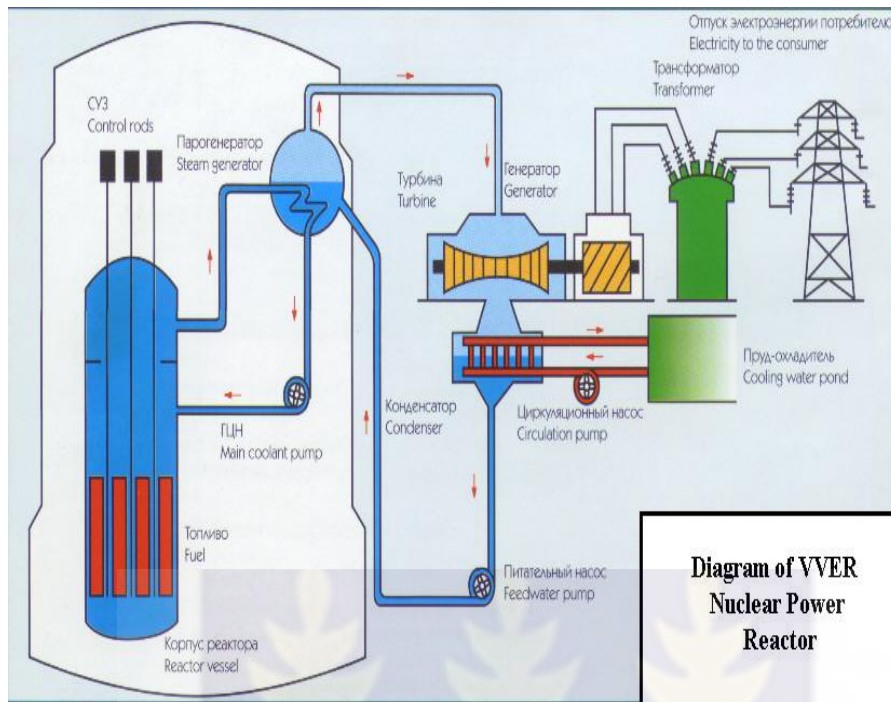


Figure 2.3 Simplified VVER-1000 plant layout

The reactor is a vertical pressurized vessel that houses the core barrel with the baffle, fuel assemblies, RCCA, and in-core instrumentation and detectors. The reactor vessel is fabricated from heat-resistant alloy steel, grade 15X2HM ϕ A chosen on the basis of mechanical properties, lack of susceptibility to brittle fracture, durability and irradiation stability (OKB GIDROPRESS, 2011).

The main coolant pipeline (MCP) connects the reactor, steam generator and main coolant pump sets between themselves forming a circulation system, and it is intended for coolant circulation through the reactor core and steam generators. The MCP consists of four circulating loops with two sections of tubes on each loop. The ‘hot’ leg is the section between the reactor outlet nozzle and the steam generator inlet collector. The section between the steam generator outlet collector and the reactor coolant pump set inlet nozzle and between RCP set outlet nozzle and the reactor inlet nozzle is the ‘cold’

leg. The internal diameter (850mm) is chosen providing the MCP acceptable pressure loss under design coolant flowrate of 21500 m³/h in each loop. The heat generated by the fission in the core is carried by the primary coolant into the steam generator to be transferred to the secondary loop via the steam exchangers. The steam generated in the secondary loop is then pumped to drive the turbines to generate electrical energy (Tikhonov, 2011).

The core is made of 163 fuel assemblies, identical in design but different in fuel enrichment, with some having 2%, 3% and 3.3% enrichment. The core has an active height of 353 cm and is made of hexagonal shaped fuel assemblies. The fuel assemblies comprise fuel rods arranged in a triangular lattice with a pitch of 1.2 cm. The core is designed for the generalized version of fuel assembly design providing its operability in using several fuel assembly types. The TVSA fuel assembly and the TVS-2 fuel assembly are designs used in the VVER core. The TVSA is a base version fuel assembly design and the TVS-2 is an alternative fuel assembly version. Both versions of fuel assemblies can be used interchangeably. Both assemblies consist of a top nozzle, bundles of fuel rods, spacer grids and a bottom nozzle. The top nozzle provides the necessary force of fuel assembly compression in the core while the bottom nozzle conjugate the fuel assembly with the support of the reactor core barrel and also guides coolant flow through the assemblies (Tikhonov, 2011). The bundle of fuel rods consist of a skeleton that houses 312 fuel rods, 20 guide tubes and spacing grids which provide strength and maintains the geometry of the fuel assemblies and fuel rods. The rod control cluster assembly (RCCA) consist of 18 absorber rods. The RCCA absorber element is a tube filled with absorbing materials such as Boron Carbide (B₄C) and dysprosium titanate (Dy₂O₃ TiO₂) and sealed.

General views of the base and alternative fuel assemblies are shown in the figure below.

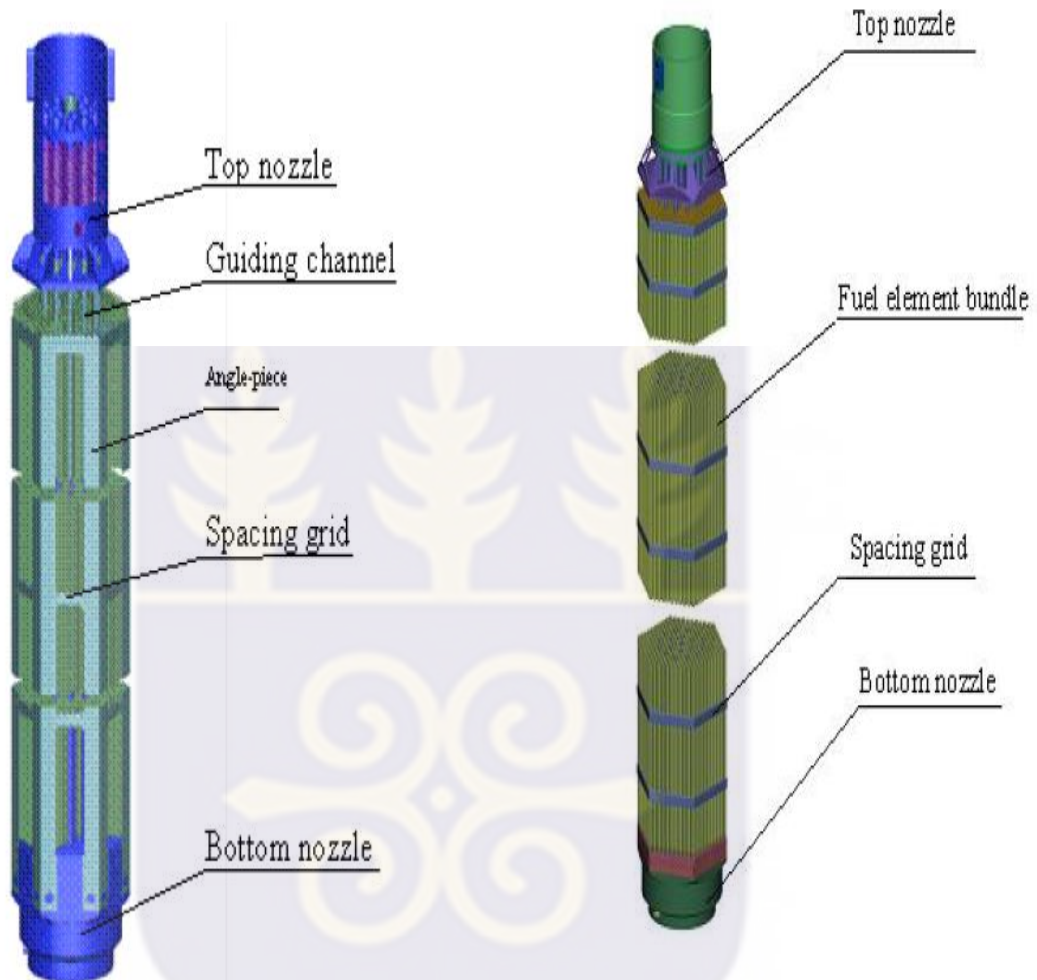


Figure 2.4a TVSA General view

Figure 2.4b TVS-2 General view

2.2.5 High Pressure Reactor (HPR1000)

The high pressure water reactor (HPR) is an active and passive advanced PWR which meets the requirements of Gen-III nuclear power plants in terms of technical maturity, safety and economic competitiveness (CNNC, 2015). The HPR-1000 was designed by the China Zhongyuan Engineering Corporation under the supervision of the China National Nuclear Corporation (CNNC).

The HPR demonstration project was commenced on the 7th of May 2015 when the China National Nuclear Safety Administration (NNSA) issued construction permission on the same day after reviewing the preliminary safety analysis report (PSAR). It is stated that “The basic safety to be achieved in the design of HPR-1000 is control of the reactivity, removal of heat from the core and spent fuel, and confinement of radioactive materials and control of operational discharges as well as limitation of accidental releases” (CNNC, 2015).

2.2.6 Design Overview of the HPR-1000

The reactor pressure vessel (RPV) is one of the most important parts in the reactor coolant system pressure boundary, and is equally significant in shielding against radioactivity. The RPV also houses the reactor core, reactor internals, core support structures and some measuring and control components. The reactor pressure vessel is composed of three parts: closure head, vessel body, fasteners and shell parts.

The reactor coolant system transports heat from the reactor core to the steam generators where the heat is transferred to the secondary system to produce steam that will be pumped to turn turbines. The reactor coolant system consists of three similar heat transfer loops connected in parallel to the reactor pressure vessel. Each loop contains a reactor coolant pump and a steam generator. During operation, the reactor coolant pumps circulate pressurized water through the reactor vessel and the coolant loops. The reactor coolant water serves as moderator and solvent for boric acid as it passes through the core (CNNC, 2015).

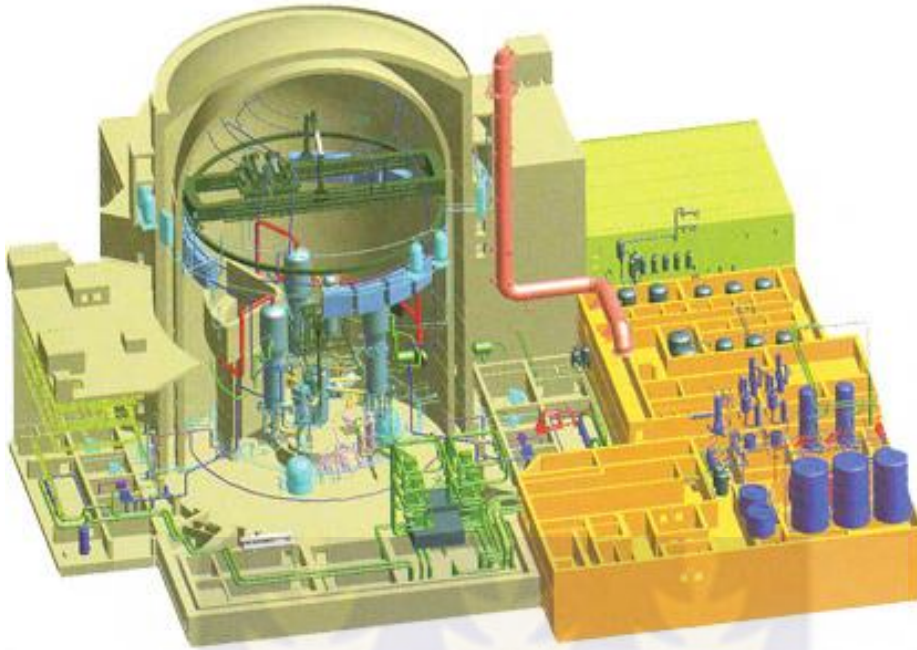


Figure 2.5 HPR plant layout

The reactor core consists of 177 fuel assemblies, which has an active core height of 365.8 cm, and an equivalent diameter of 322.8 cm. Fuel assemblies of three enrichment are used in the initial core, which are 1.8%, 2.4% and 3.1% respectively. Two regions consisting of the two lower enrichment are interspersed so as to form a checker board pattern in the central portion of the core. The third and highest enrichment is arranged around the periphery of the core.

The core is designed to be loaded with the China Fuel (CF) series, precisely the CF3 fuel assembly. The CF3 fuel assembly is composed of 264 fuel rods arranged within a 17x17 supporting structure. The supporting structure (skeleton) is made of 24 guide thimbles, 1 instrumentation, a top and bottom nozzle, 8 grids and 3 mid-span mixing grids.

Fuel rods are slightly enriched sintered uranium oxide pellets contained in a closed tube, hermetically sealed at its ends by wedged end plugs. The gap between the pellet and the cladding, the initial pressurization and density of the pellets are calculated so as to minimize interaction between the pellet and the cladding (PCI). The guide thimbles are structural members which also provide channels for the control rods, neutron absorber rods, burnable poisons rod (for the first core), and neutron source or thimble plug assemblies.

Also among the core components are the rod control cluster assembly made up of a group of individual neutron absorber rods fastened at the top end to a common spider assembly. The RCCA are used to for shutdown and control purposes to offset fast reactivity changes.

2.3 Overview of Neutronic Safety Parameters of Nuclear Reactors

The performance of a nuclear reactor principally depends on the behaviour of neutrons in the core. The interactions of neutrons with core materials bring about several effects such as; nuclear fission, heat generation, and induced radioactivity in reactor materials. These effects, lead to various reactor aspects such as reactivity control, reactor kinetics, xenon stability, fuel depletion, and isotope production which play an integral part in the quest to understanding reactor performance and safety. The distribution of neutrons in the core plays a central role in establishing a power distribution, heat transfer profile and safe operation of the reactor. There are strong feedback effects between nuclear physics and the other physical processes in the reactor, particularly safety (Zohuri, 2016).

Multiplication factor (k) is the ratio of the number of neutrons in one generation to the number of neutrons in the preceding generation. If k is smaller than 1.0, it means that number of neutrons is decreasing, so reactor will shut down itself automatically a period later. If k is greater than 1.0 it means number of neutrons is increasing, so power will increase exponentially. Consequently, unless multiplication factor is equal to 1.0, reactor will not work at steady state conditions. This is the “criticality condition” which is the basic design parameter of a nuclear reactor.

A study of criticality safety and neutronic performance for a 348-fuel pin Ghana Research Reactor-1 LEU core using MCNP code was carried out by Odoi *et al*, 2014. The MCNP5 transport code was used to perform the Monte Carlo calculations. Nuclear data for fissile and non-fissile isotopes associated with materials (fuel and clad, coolant, moderator, control rod and clad, reflectors, 5 structural components) of the physical model was chosen from ENDF/B-VI nuclear data libraries. The Criticality results for the HEU and 348-pin LEU cores were given as $k_{\text{eff}} = 1.00375 \pm 0.00005$, $\rho = 3.74 \pm 0.05$ and $k_{\text{eff}} = 1.00385 \pm 0.00004$, $\rho = 3.84 \pm 0.0$. The Multiplication factors, k_{eff} , and the reactivities were reported to be quite comparable and also compared well with values stated in the HEU SAR as reported by Odoi *et al* (Odoi, Akaho, Jonah, Abrefah, & Ibrahim, 2014).

In a neutronics calculation performed by Mahlers, the MCNP code based on the Monte-Carlo method was applied. Continuous-energy cross-sections for use with MCNP were calculated with the NJOY code. Calculated criticality, pin-to-pin power distribution, time-dependent critical concentration of soluble boron, worth of the control rods, average fuel assembly powers and time-dependent axial power distribution were compared to the corresponding experimental values for both zero-power VVER-1000

model, created at the LR-0 experimental facility, and the first fuel cycle of a real VVER-1000 reactor. For all of these parameters, it was concluded that neutronics calculation with ENDF/B-VII is in good agreement with the experimental measurement. Moreover, for VVER-1000 neutronics calculation, ENDF/B-VII provides better results than ENDF/B-VI” as reported by Mahlers (Mahlers, 2009).

Balaceanu *et al* in a study intended to highlight a global neutronic calculation system by using it to estimate the neutronic effect of the adjuster rod system insertion in the CANDU Standard core. The calculation system WIMS_PIJXYZ_LEGENTR is based on transport methods and was developed in the Institute for Nuclear Research Pitesti. These results are compared with the similar ones obtained by the WIMS_PIJXYZ_DIREN calculation system. The k-eff obtained for the CANDU from the study was 1.0348 and was compared to the reference k-eff of the CANDU reactor, which is 1.0527. This confirmed that it was a coherent and consistent methodology which can be used successfully for estimating the global neutronic parameters specially for the CANDU reactor core as concluded by the study (Balaceanu & Pavelescu, 2010).

Ghana currently operates a research reactor, which is a Miniature Neutron Source Reactor (MNSR) similar to the Canadian SLOWPOKE.

Neutron flux is a very important parameter in utilizing and optimizing MNSR facilities. In neutron activation analysis, radioisotope preparation, material testing and other uses of the MNSR, neutron flux is key. For neutron activation analysis for instance, a minimum neutron flux of about 10^9 to 10^{10} n/cm²/s is required. For research reactors, much safety is assured when there is prompt and inherent reactivity feedback associated with the design. The negative reactivity temperature coefficient (RTC) is a design provision in the MNSR and SLOWPOKE reactors that gives them inherent safety

features. Therefore, reactivity is affected in these reactors by other factors such as expansion in fuel and moderator, void production, etc.

In nuclear power reactors, changes of temperature affect the reactivity in many ways. Changes in reactivity due to moderator temperature changes, fuel temperature changes and changes in void content make up the total reactivity coefficient. In PWRs working at steady state, the change in reactivity due to moderator temperature changes is the most important. Reactivity changes due to change in void content is less significant in a PWR working at steady state, however, this become very necessary when simulating a loss of coolant (LOCA) situation. Overall, the contribution of the fuel temperature of reactivity to the total is very small but the fluctuation in temperature gives information on fuel oscillation (Aguilar & Por, 1987).

2.3.1 Void Coefficient

Void formation inside the reactor core is a well-known and thoroughly studied phenomenon. A void present in a reactor influences its reactivity. It can appear in the moderator and/or coolant because of steam formation, which has a density of several orders of magnitude smaller than that of the liquid. The void coefficient of reactivity is a physical quantity, describing the sign and magnitude of the reactivity change of a nuclear reactor as void (typically steam bubbles) forms in the reactor moderator or coolant. Reactors with a liquid coolant and moderator will have either a negative void coefficient of reactivity (under-moderated reactor) or a positive void coefficient (over-moderated reactor). Below is a typical graph which shows the effect of varying void fraction on the reactivity.

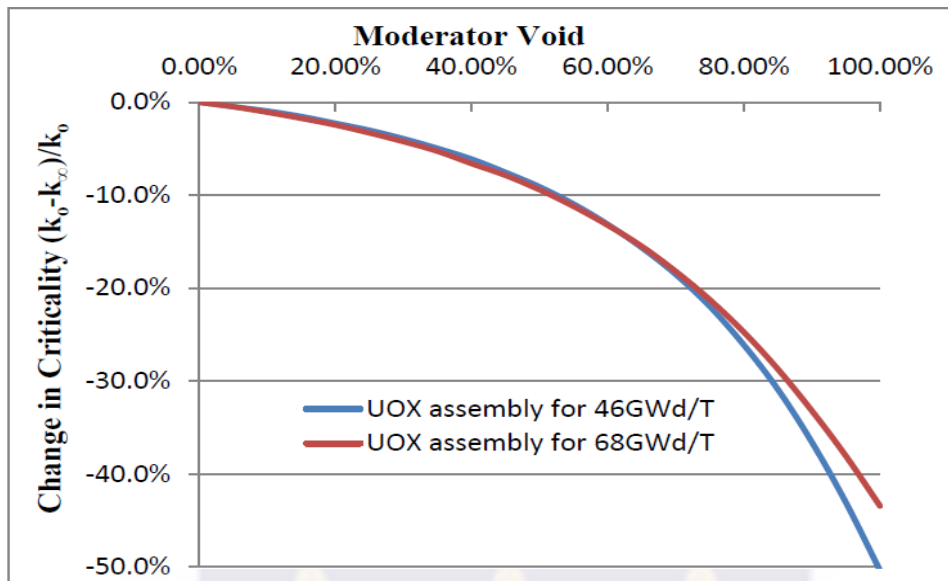


Figure 2.6 Plot of Reactivity against Moderator Void Fraction for a typical French EPR (Sogbadji, 2012)

Jazbec *et al*, 2013, employed the Monte Carlo neutron transport code MCNP to simulate the effect of the void and to calculate the activation of air going through the core of the Jozef Stefan Institute TRIGA reactor. The results showed that the system is safe and that operation under normal and accident conditions does not lead to violation of operational limits and conditions of the reactor. Results of the study showed that the void coefficient is not depended on the volume of void, it is independent on the water density. Its value is about -99.6pcm/% (Jazbec, Snoj, & Kavšek, 2013).

Khan *et al*, 2011, used the Monte Carlo neutronics simulating code, equipped with the cross sections library JEFF 3.1, to determine the reactivity coefficient of the TRIGA Mark II research reactor. For each execution, the void sample was moved 5cm up in axial direction. From the output, effective multiplication factor k_{eff} for each run was obtained to calculate the corresponding reactivity effect in dollars the using effective delayed neutron fraction $\beta = 0.0073$. From the results, it is observed that

reactivity coefficient ranges from -0.044 to 0.073 cents per cubic centimeters in the TRIGA reactor. In contrast to other water-moderated reactors, the effect of void compensates the negative reactivity introduced due to decrease in moderation (Khan, Villa, & Bock, 2011).

2.3.2 Temperature Reactivity Coefficient

Knowledge of the changes in reactivity with respect to temperature is relevant in providing information on the safety analysis at all reactor operation conditions. Reactivity and power excursion transient analysis is very much dependent on the temperature reactivity coefficients. In the studies of reactivity coefficients, great importance is attributed to the sense, magnitude and response time of the reactivity change (Faghihi, Fadaei, & Sayareh, 2007).

Temperature reactivity coefficients are of two main forms; the fuel temperature reactivity coefficient and the moderator temperature reactivity coefficient. The time required for a change in reactivity with a change in fuel temperature is short hence the fuel temperature reactivity is considered a prompt reactivity coefficient. On the other hand, the time taken for a change in reactivity with change in moderator temperature is much longer hence the moderator temperature reactivity is a delayed coefficient (Lamarsh R. J., 1982). To measure the temperature reactivity coefficient, the change in reactivity is observed when the core temperature is raised. This is done at a given power level while all other operational parameters are kept constant. The fuel type, enrichment, core fuel loading, burn-up poison concentration and temperature distribution in different regions influence reactivity in the core. Taking into consideration all these factors, the reactivity can be accurately estimated. Reactivity changes with respect to moderator temperature changes is depicted in the figure below.

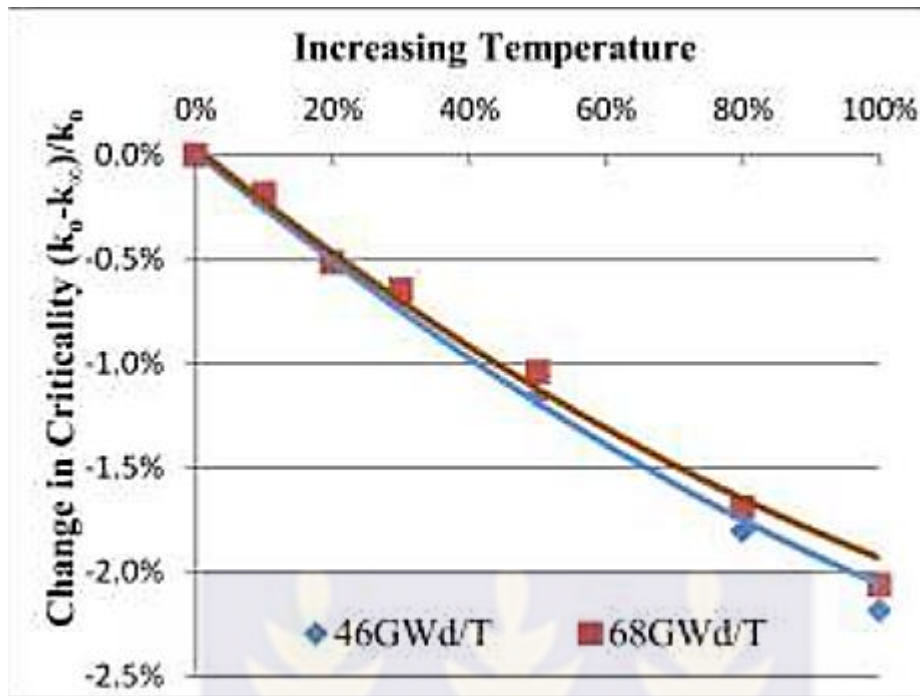


Figure 2.7 Change in Reactivity against Moderator Temperature for a typical French EPR (Sogbadji, 2012)

Alhassan *et al*, 2010, in The Analysis of the Reactivity Temperature Coefficient (RTC) of the Ghana Research Reactor-1 using the reference HEU-UAl₄ and then the LEU-UO₂ fuel currently being developed under the RETR programme was carried out to determine the Fuel Temperature Coefficient (FTC) and Moderator Temperature Coefficient (MTC) using SCUBA, a locally developed FORTRAN 95 code. The temperature effects on the thermal fission factor (η) and the thermal utilization factor (f) were analysed to determine the contribution of each isotope present in the fuel cell to reactivity temperature coefficient. From the study, it was reported that the average values of the core RTC for the temperature range of 15°C to 140°C at the beginning of life of the core were observed to be -0.70×10^{-4} and -2.061×10^{-4} for the HEU-UAl₄ and the LEU-UO₂ respectively.

Safarzadeh *et al*, 2015, conducted a study in “Calculation of reactivity coefficients with burn-up changes for VVER-1000 reactor”. The influence of burn-up, fission product

build-up and fuel depletion were considered in determining the coefficients. Reactivity changes due to boric acid concentration and moderator density were also computed. To perform the neutronic calculations, the reactor core was simulated using DRAGON4 and DONJON4 codes. The thermal-hydraulic (T-H) calculation was performed using single heated channel model. The T-H model is implemented for VVER-1000 reactor as a computer program. These codes are coupled by development of an auxiliary computer program. The obtained results are compared with the plant's FSAR that confirm the ability and reliability of the method (Safarzadeh, Saadatian-Derakhshandeh, & Shirani, 2015).

Aguilar *et al*, 1987, in a study entitled; “Monitoring Temperature Reactivity Coefficient by Noise Method in NPP at full Power.”. This made it possible to measure its dependence on boron concentration. “The method gives good results and can thus be applied for permanent monitoring of this safety parameter” according to Aguilar *et al* (Aguilar & Por, 1987).

A theoretical study of reactivity coefficients analysis of the Bushehr Nuclear Power Plant (BNPP), VVER-1000, at nominal conditions was carried out during its first operational cycle where WIMS and CITATION codes were used by Faghihi *et al*, 2007. Modelling of all rods (including fuel rods, control rods, burnable and non-burnable poison rods) and channels (including central guiding channel, central channel and reactor perimeters) were carried out using the WIMS code. Modelling of the fuel assemblies and reactor core was achieved using the CITATION code. The multi-group constants generated by WIMS for different fuel configurations were fed into CITATION. The multi-group constants for fuel assemblies are obtained from the flux distribution calculated by the code. A FORTRAN 90 program is written to link the

WIMS and CITATION codes to facilitate their numerous executions. The calculated reactivity coefficients were comparable with the plant's FSAR. The results of the study showed that, temperature increase would increase negative reactivity insertion and negative coolant temperature coefficient of reactivity increases during the cycle due to the decrease in boric acid concentration. (Faghihi, Fadaei, & Sayareh, 2007).

2.4 Concluding Remarks

Several different computer codes have been used to carry out studies similar to this work in other reactors. The Monte Carlo N-Particle code (MCNP5) is employed to achieve the results in this research. The MCNP theory and technique is discussed in the next chapter. The chapter gives further insight into how the neutrons are treated in the fuel assembly and the advantages of the Monte Carlo statistical approach compared to other methods.



CHAPTER THREE

3.0 THEORITICAL ANALYSIS

3.1 Introduction

This chapter and the subsequent sections introduce the theory relevant to Monte Carlo techniques and neutron transport. The chapter also covers basic nuclear reactor theory and the required reactor physics.

The technical and design specifications of reactor core determine the behaviour of the neutrons in the reactor hence the criticality conditions and the total power of the reactor (Lamarsh & Baratta, 2012). This is essential to the design of every reactor. In particular, the design of a nuclear reactor is based on the interaction of several variables including fuel type, the moderator and coolant, core geometry and composition, radiation shielding, thermal hydraulics, criticality and reactor safety.

3.2 Nuclear Reactor Theory

In a steady state radiation field, the net rate at which particles are lost in an element must be exactly balanced by the rate of secondary or source particles which are introduced into the volume. The linear particle transport equation or linearized Boltzmann transport equation is used to determine the particle distribution in space, r direction, Ω and energy, E in plane, spherical or cylindrical geometry. The equation is the basic physical model to describe the transport of uncharged particles such as photons (γ – rays, light, etc.) and neutrons.

Calculations of conditions necessary for criticality are normally carried out using the group diffusion method. The one-group diffusion method gives only the roughest estimates of the properties of a critical reactor and is most appropriate for a fast reactor

(Larmash R. J., 2001). For convenience, all materials other than the fuel are considered as moderator for one-group calculations. The thermal reactor system contains fuel, coolant, various structural materials, and a moderator to slow down the fission neutrons to thermal energies. The several regions with different material properties are represented by a set of equations. In this case, it is important to solve the equations in each region and satisfy the boundary conditions at every interface and at the reactor surfaces. To obtain accurate results, the multigroup diffusion method is employed. The procedure can only be carried out in a practical way with a high-speed computer, and there are many computer programs written for solving the multigroup equations (Larmash R. J., 2001).

3.3 Neutron Transport Theory

The physics of the requirements of a nuclear reactor core is determined by the description of production, transport and absorption of neutrons in the core. Neutrons move about in a reactor in complicated paths due to repeated collisions with nuclei, making it difficult to predict the distribution of neutrons in space, energy and time. The equation governing this neutron transport phenomenon is called the neutron transport equation, which expresses the distribution of neutrons in space, energy and time in a straightforward manner. The transport equation is fundamental to calculating the conditions necessary for criticality in a reactor, the spatial distribution of neutron flux at various energies and other quantities which form the basis of nuclear reactor design. In principle, the prediction of the distribution of neutrons can be done by solving the neutron transport equation. Various approximations are used and numerical solutions are obtained by computational procedures. The general form of the transport equation can be written as (Glasstone & Sesonske, 1994);

$$\left[\begin{array}{c} \text{change in} \\ \text{neutron density} \\ \text{with time} \end{array} \right] = \left[\begin{array}{c} \text{change due to} \\ \text{physical changes} \end{array} \right] + \left[\begin{array}{c} \text{change due} \\ \text{to collision} \end{array} \right] + \left[\text{sources} \right] \quad (3.1)$$

This is expressed mathematically as:

$$\frac{1}{v} \frac{\partial}{\partial t} \phi(\vec{r}, \hat{\Omega}, E, t) = -\Omega \cdot \nabla \phi(\vec{r}, \hat{\Omega}, E, t) + S(\vec{r}, \hat{\Omega}, E, t) - \Sigma_t(\vec{r}, E, t) \phi(\vec{r}, \hat{\Omega}, E, t) + \int_0^\infty dE' \int_{4\pi} d\Omega' \Sigma_s(\vec{r}, E' \rightarrow E, \hat{\Omega}' \rightarrow \hat{\Omega}, t) \phi(\vec{r}, \hat{\Omega}', E', t) \quad (3.2)$$

where

$\phi(\vec{r}, \hat{\Omega}, E, t)$ = the expected number of particles per unit time at r with energies in unit energy about E and moving in a unit angle about Ω ,

$S(\vec{r}, \hat{\Omega}, E, t)$ = the number of source particles emitted in a volume dV travelling in a cone of direction $d\Omega$ about Ω with energies between E and dE

$\Sigma_s(\vec{r}, E' \rightarrow E, \hat{\Omega}' \rightarrow \hat{\Omega}, t)$ = macroscopic scattering cross-section which is the probability that the particles at position r with energy E' travelling in the direction $\hat{\Omega}'$ scatter into dE about E and into the cone of direction $d\Omega$ about $\hat{\Omega}$

The corresponding steady state equation is

$$[\hat{\Omega} \cdot \nabla + \Sigma_t] \phi(\vec{r}, \hat{\Omega}, E) = \int dE' \Sigma_s(\vec{r}, \hat{\Omega}' \rightarrow \hat{\Omega}, E' \rightarrow E) \phi(\vec{r}, \hat{\Omega}', E') d\Omega' dE' + S(\vec{r}, \hat{\Omega}', E') \quad (3.3)$$

The neutron transport equation holds under some strict assumptions such as (Miller & Lewis, 1993):

- The particles are treated as points.
- Between any two points, particle motion is in straight line.
- Interactions between particles are not considered.

- Collisions are prompt.
- Isotropic properties are assumed for the material.
- Material composition and nuclei properties are known and time dependent.
- The particle density distribution is the mean value.

3.4 Methods Used to Solve or Simulate Neutron Transport

There are several computational codes available for use in light water reactor analysis.

A survey of literature is done to investigate the capabilities of these codes for applications in the reactors under consideration. The different methods applied to neutronic codes are studied to identify a code for modelling the HPR, EPR and VVER.

3.4.1 Deterministic Methods

Deterministic methods basically solve the neutron transport equation for the average particle behaviour. A deterministic model has no stochastic elements and the entire input and output relation of the model is conclusively determined.

I. Diffusion Methods

Diffusion theory, with flux reconstruction, is the present state of the art for reactor physics analysis and design. The diffusion theory method based codes solve the neutron diffusion equation to obtain the neutron flux, from which the power profile is determined. They use macroscopic cross-section data from two or more energy groups for neutron particles. Diffusion codes have been used to study reactors with appropriately homogenised fuel, moderator and absorbing material distribution. However, for a very heterogeneous system like the fuel assemblies and core under consideration, the simplified model will require a lot of homogenisation techniques and calculations. Examples of diffusion codes are given as follows.

DYN3D is a neutron kinetic code used for calculation of transients in LWR cores (Kotlyar, Shaposhinik, & Frindman, 2011). PANBOX is a multidimensional neutron kinetics code developed to perform safety and transient analysis of PWR (Sanchez & Hering, 2002).

II. Other Methods

Only discrete ordinate methods are discussed in this section because it is the most common. The discrete ordinate method sees the geometry or phase space to be divided into many volumes and angles. The neutron transport equation is then solved in terms of the volumes and discrete angles. If this method is used to model the VVER, HPR or EPR core, the moderator, fuel rods, guide tubes and instrumentation tubes will be homogenised for each volume and angle to be able to solve the transport equation.

Examples of these codes are discrete ordinate codes DORT, TORT and DORT-TD

DORT is a two-dimensional (X-Y and R-Z) code while TORT is a three-dimensional discrete transport code (Pautz, Hasse, & Zwermann, 2005) and DORT-TD is a transient neutron transport code (Waata, 2006).

3.4.2 Stochastic Methods

Stochastic methods or Monte Carlo do not solve the transport equation like the deterministic method based codes mentioned above, but rather simulate particle transport for each particle by tracking the path of each individual particle throughout its life time and records (tallies) the average behaviour of these particles. Monte Carlo codes use given libraries e.g. ENDF cross-section data of continuous energy.

Monte Carlo codes are used because of their ability to model complex geometries and the accuracy of solutions produced with the ENDF continuous energy cross-section

data. Hence the reason MCNP5 was chosen to be used for this study despite the MCNP5 drawbacks such as extensive calculation time and computational memory required per calculation. However, it should be noted that this does not imply that MCNP is better than other methods.

Monte Carlo based computer codes include Monte Carlo N-Particle (MCNP). This is a general-purpose, continuous-energy, generalised-geometry, coupled neutron/photon/electron transport code (X-5 Monte Carlo team., 2003). However it should be noted that energy group collapsed cross-section data can also be used in MCNP. Section 2.4 further discusses the Monte Carlo technique and MCNP5.

3.5 Monte Carlo Technique

A Monte Carlo based code MCNP5 is used to calculate neutron flux, fission energy and heating energy deposition in the fuel assemblies from fission. It should be noted that non-local gamma heating is not taken into account in this work. The F7 tally includes only local gamma-ray heating. This fission energy and heating energy corresponds to the power distribution in the fuel assemblies. The power distribution is obtained as a function of axial height and radial distance (X-5 Monte Carlo team., 2003). An introduction to the Monte Carlo technique is described in the section to provide better comprehension of the modelling.

The fundamental idea of Monte Carlo is to create a series of histories of particle life (neutrons) by using statistical sampling techniques to sample the probability laws that describe the behaviour of neutrons and trace the particle events steps by step till the death of the particle. Monte Carlo techniques are based on statistical concepts; this implies that the result given is an estimate and should lie on some confidence interval

about the true answer. The statistical error or rather the uncertainty associated with the result and the confidence interval is a function of the number of particle histories simulated. The more histories run the smaller the confidence interval about the true behaviour of the particles. According to the central limit theorem the estimated quality will improve with increase in sample size. For example, a Monte Carlo simulation outputs successive independent scores, x_1, x_2, \dots, x_n of a random variable x . Then the sample mean (\bar{x}) is formed where N is the total number of histories (MCNP5, 2003).

$$\bar{x} = \frac{1}{N} \sum_{i=1}^N x_i \quad (3.4)$$

The law of large number states the sample mean with a probability that approaches 1 as $N \rightarrow \infty$ approaches the population mean or true mean. In this case x may represent the neutron flux, heating energy deposition, fission energy deposition, k_{eff} etc (Motwendi, 2014).

3.5.1 MCNP Tallies

Note that a tally refers to counts that are kept by MCNP. In MCNP there are seven types of tallies present. They include six standard neutron tallies, six standard photon tallies and four standard electron tallies (X-5 Monte Carlo team., 2003). The standard tallies can be modified by the user in many ways. All the tallies are normalised to be per starting particle except for the KCODE criticality problems, which are normalised to be per fission.

For this study only neutron tallies are used, so only neutron tallies will be discussed.

These tallies are the F4: N tally which is the track length estimate of cell flux and F7:

N which is the track length estimate of the fission energy deposition as described below.

Tally Mnemonic	Description
“F1:N or F1:P or F1:E”	Surface current
“F2:N or F2:P or F2:E”	Surface flux
“F4:N or F4:P or F4:E”	Track length estimate of cell flux
“F5a:N or F5a:P”	Flux at a point or ring detector
“F6:N or F6:P or F6:N,P”	Track length estimate of energy deposition
“F7:N”	Track length estimate of fission energy deposition
“F8:N or F8:P or F8:E”	Pulse height tally

3.5.2 Neutron Flux and Power Distribution

The MCNP is used to simulate average behaviour of neutron particles in the material contained in the geometry cells. These neutrons are tracked with ENDF/B (evaluated cross section data files); however, it is important to note that the ENDF/B is not the only cross-section library used in MCNP. Other data libraries that might be used in MCNP are the European JEF-2.2 library, the Japanese Atomic Energy Institute’s JENDL library, the Chinese Data Center’s CENDL library and the Russian BOFOD library. The neutron tracks recorded represent the neutron flux distribution and are multiplied with reaction cross-sections track by track and with fission functions to obtain an estimate of the fission energy, which corresponds to power distribution. The F4 tally which represents the track length estimate of the cell flux is defined as:

$$\frac{1}{V} \int_V dV \int_E dE \int_t dt \phi(\vec{r}, E, t) = \frac{W_t T_l}{V} \quad (3.5)$$

Where;

W_t = Particle weight

T_l = Track length (cm)

V = Cell volume (cm³)

ϕ = Neutron flux (neutrons/cm²-s)

The flux can be obtained from the fluence tally for a time-dependent source by dividing the tally by the time bin width. These tallies can all be made per unit energy by dividing by the energy bin width (X-5 Monte Carlo team., 2003).

3.5.3 Cross-Section Data

The MCNP code package is incomplete without the associated nuclear data tables. The kinds of tables available and their general features are outlined in this section. How to use the MCNP data tables is described in this Section. The cross section data available to the MCNP reproduces the original evaluated data and physical properties of the materials as much as it is practical. New cross section data can be brought into the MCNP package in a timely fashion, thereby allowing most recent evaluations.

Nuclear cross-section data describe the frequency and outcome of interactions between particles (neutrons) and materials through which they are traversing. The type of nuclear data used in MCNP is point-wise cross-section data. Nuclear data in this form are stored at a significantly large number of energy points such that the point-wise data retain the particle energy as a continuous variable. The cross-section data for neutrons interaction is obtained from the evaluated MCNP libraries ENDF/B. The cross-section data provided for MCNP are evaluated at set temperatures (MCNP5, 2003).

Each data table is identified by a ZAID. The general form of a ZAID is $ZZZAAA.nnX$, where ZZZ is the atomic number, AAA is the atomic mass number, nn is the unique evaluation identifier, and X indicates the class of data. For elemental evaluations $AAA=000$. Data tables are selected by the user with the Mn, MPNn and MTn cards (MCNP5, 2003).

3.5.4 Determination of Fission Cross Section

Fission cross-section σ_f is defined as a measure of the probability that a neutron and a nucleus interact to form a compound nucleus which then undergoes fission (Stacey, 2007). Total cross-section is defined by neutron interactions scattering σ_{sca} and absorption σ_a

$$\sigma_{tot} = \sigma_{sca} + \sigma_a \quad (3.6)$$

The scattering and absorption can both be sub-divided into further parts

$$\sigma_{sca} = \sigma_{non-elastic} + \sigma_{elastic} \quad (3.7)$$

and

$$\sigma_a = \sigma_f + \sigma_\gamma + \sigma_a^{other} \quad (3.8)$$

where σ_a^{other} refers to other absorption reactions such as n,n and n,2n reactions.

Substituting (3.6) and (3.7) into (3.8) and rearranging gives

$$\sigma_f = \sigma_{tot} - (\sigma_{sca} + \sigma_\gamma + \sigma_a^{other}) \quad (3.9)$$

3.5.5 Treatment of Thermal Neutrons

A collision interaction between a neutron and an atom is dependent on the thermal motion of the atom and in many instances it is also affected by the presence of other atoms next to it. In MCNP, the thermal treatment is based on the free gas approximation to account for the thermal motion. MCNP also has capabilities of using an explicit thermal scattering $S(\alpha, \beta)$ that accounts for the effect of chemical bonding and crystal structure for incident neutron energies less than 4eV. The shortcoming of the $S(\alpha, \beta)$ is that data are available for a limited number of materials and temperatures. Because of lack of cross-section data, the free gas model can be used for treatment of the thermal neutrons. With the free gas model MCNP assumes that the hydrogen is a free gas. Since most of the scattering of fast neutrons is due to hydrogen the results should be significantly close.

In the range of atomic weight and neutron energy where thermal effects are significant the elastic scattering cross-section is almost independent of the energy of the neutron and the reaction cross-sections are nearly independent of the temperature.

The free gas model in MCNP is included by using a temperature card “tmp card” in the input file (Mattes & Keinert, 2005).

3.5.6 Criticality Calculations

The effective multiplication factor k_{eff} is generally defined as the product of P_{NL} and k_{∞} which is the total number of fission neutrons produced on average by one neutron from the previous fission event:

$$k_{eff} = \eta f \epsilon \rho P_{NL} \equiv k_{\infty} P_{NL} \quad (3.10)$$

where:

k_{∞} = k -infinity for infinite systems

η = Reproduction factor

f = Fuel utilization factor

ε = Fast fission factor

ρ = Resonance escape probability

P_{NL} = Non leakage probability

The equation (3.10) is further expanded and explained in nuclear reactor physics book. (Glasstone & Sesonske, 1994), (Lamarsh & Baratta, 2012) and (Stacey, 2007).

In MCNP, the calculation of the multiplication factor is obtained by the use of a criticality calculation. The k_{eff} in MCNP is defined as the ratio of neutrons in one generation to the number of neutrons in the generation preceding it in a system containing fissile material and with no external sources.

A generation is the neutron lifetime from birth in fission to death by leakage, parasitic capture or absorption to fission. In MCNP, neutron generations are referred to as cycles.

$$k_{eff} = \frac{\text{fission neutrons in generation } i+1}{\text{fission neutrons in generation } i} \quad (3.11)$$

For critical systems, $k_{eff}=1$ this implies that the fission reaction will be able to sustain itself. For sub-critical systems, $k_{eff} < 1$ this implies that the neutrons born are less than neutrons dying hence the fission reaction is not self-sustaining. For super-critical systems, $k_{eff} > 1$ this implies that the number of neutrons will increase due to more neutrons being born from the fission reaction.

Nuclear reactor criticality is a very important activity required in the analysis involving reactor design, reactor operation and safety. Hence the effective multiplication factor in Monte Carlo criticality applications is of primary interest. In these calculations, a group of neutron histories is often referred to as a k_{eff} cycle with the multiplication of the assembly defined by the ratio of the number of neutrons generated at the end of k_{eff} cycle to the number of neutrons whose histories are evaluated in this cycle. The expected value of the multiplication factor is then estimated by averaging over the events in the k_{eff} cycle.

3.5.7 Convergence

Monte Carlo based calculations such as criticality (k_{eff}) calculations are based on iterations. The fission source distribution and an estimated value for k_{eff} are specified by the user. Random walks of a single-generation of neutrons are carried out for each cycle to estimate the new value of fission source distribution of the next generation. The iterative process is repeated until both k_{eff} and fission source distribution has converged. Results obtained before this point are set as inactive. Only after convergence tallies are initiated and the iterations are continued until statistical uncertainties are acceptably small. That is why there is a need to divide the cycles into two, these being the inactive and active cycles. The inactive cycles are before convergence and active cycles are post convergence of the k_{eff} and the fission source distribution (H_{src}) where Monte Carlo tallies are accumulated.

Determination of convergence in Monte Carlo criticality calculations is made difficult by inherent statistical noise of neutron random walks in each generation (Brown, 2006). Historically, convergence in MCNP (MCNP5, 2003) and other codes was determined

by performing a preliminary calculation from which post-processing is done to assess trends in k_{eff} . After determining the inactive and active cycles, the calculation is then repeated and results are obtained. This can become a problem because convergence of k_{eff} happens before the fission source distribution converges, so the testing should also include both k_{eff} and the fission source distribution using the Shannon entropy estimation capabilities built in MCNP5.

3.5.8 Theory of Convergence of k_{eff} and Fission Source Distribution

The neutron transport equation is employed to further explain the convergence in k_{eff} .

From the transport equation k_{eff} can be written in standard form as follows (Brown, 2005):

$$[\Omega \cdot \nabla + \Sigma_t(\vec{r}E)]. \Psi(\vec{r}, E, \hat{\Omega}) = \iint \Psi(\vec{r}, E', \hat{\Omega}') \Sigma_s(\vec{r}, E' \rightarrow E, \hat{\Omega}, \hat{\Omega}') d\hat{\Omega}' dE' + \frac{1}{k_{eff}} \frac{\chi(E)}{4\pi} \iint v \Sigma_F(\vec{r}, E') \Psi(\vec{r}, E', \hat{\Omega}') d\hat{\Omega}' dE' \quad (3.12)$$

where:

k_{eff} = Eigen value for fundamental mode

$\Omega \cdot \nabla \Psi(\vec{r}, E, \hat{\Omega})$ = the loss term, leakage

$\Sigma_t(\vec{r}E) \Psi(\vec{r}, E, \hat{\Omega})$ = the loss term, collisions

$\iint \Psi(\vec{r}, E', \hat{\Omega}') \Sigma_s(\vec{r}, E' \rightarrow E, \hat{\Omega}, \hat{\Omega}') d\hat{\Omega}' dE'$ = the gain term, scatter from $E', \hat{\Omega}'$ into $E, \hat{\Omega}$

$\frac{1}{k_{eff}} \frac{\chi(E)}{4\pi} \iint v \Sigma_F(\vec{r}, E') \Psi(\vec{r}, E', \hat{\Omega}') d\hat{\Omega}' dE'$ = the gain term from fission.

The equation (3.12) above is simplified using operators and written as

$$(L + T)\Psi = S\Psi + \frac{1}{k_{eff}} F\Psi \quad (3.13)$$

And rearranged to

$$\Psi = \frac{1}{k_{eff}} (L + T - S)^{-1} M \Psi = \frac{1}{k_{eff}} F \Psi \quad (3.14)$$

Equation (3.13) can be solved using a standard method as in (Brown, 2005)

$$\Psi^{(n+1)} = \frac{1}{k_{eff}^{(n)}} F \Psi^{(n)}, \quad n = 0, 1 \quad \text{given } k_{eff}^0 \Psi^0 \quad (3.15)$$

For convergence of k_{eff} and fission source distribution during the power iteration process, if expansion of $\Psi^{(0)}$ is done in terms of the eigenvectors \vec{u} , as $\Psi = \sum_{j=0} a_j^0 \vec{u}_j$ and substituting into (3.14) and rearranging algebraically to give

$$\Psi^{(n+1)}(\vec{r}) = \vec{u}_0(\vec{r}) + \frac{a_1}{a_0} \rho^{(n+1)} \cdot \vec{u}_1(\vec{r}) + \dots \quad (3.16)$$

$$k_{eff}^{(n+1)} = k_0 \left[1 - \frac{a_1}{a_0} \rho^n (1 - \rho) g_1 + \dots \right] \quad (3.17)$$

where ρ is the dominance ratio (k_1/k_0), k_0 and \vec{u}_1 are the fundamental mode eigenvalue (exact k_{eff}) and eigenfunction, k_1 and \vec{u}_1 are the first higher mode eigenvalue and eigenfunction, and a_0 , a_1 and g_1 are constants obtained from expansion of the initial fission distribution. Equation (3.16) shows that the higher-mode noise in the fission distribution disappears as $\rho^{(n+1)}$, whilst higher-mode noise in k_{eff} disappears as $\rho^n (1 - \rho) g_1$. When the dominance ratio approaches 1, k_{eff} converges before fission source distribution because of the extra dumping factor $(1 - \rho)$ that is close to zero (Brown, 2005). Hence the importance of monitoring convergence of both k_{eff} and the fission source distribution.

3.6 Estimation of Monte Carlo Precision

Monte Carlo results are an average of contributions from a lot of histories sampled during the cause of the problem. A quantity equally important as the Monte Carlo result

is the error or uncertainty associated with the result. The behaviour of the error versus the number of histories gives insight into the quality of the result and determines whether the tally is statistically well-behaved. If the tally result is not well-behaved its estimated error may not reflect its true confidence interval and the answer could be completely wrong.

A number of quantities are present in MCNP to help assess the quality of the confidence interval of a tally result. These quantities are the estimated mean, relative error, variance of variance and history score probability density.

3.6.1 Estimated Mean

Monte Carlo results are obtained by sampling random walks and assigning a score x_i to each random walk.

Assume $f(x)$ is the history score probability density function for selection of a random walk that scores x to the tally being estimated. The true mean is the expected value of x , $E(x)$, where

$$E(x) = \int x f(x) dx = \text{true mean} \quad (3.18)$$

The true mean is then estimated by the sample mean \bar{x} where

$$\bar{x} = \frac{1}{N} \sum_{i=1}^N x_i$$

The quantities $E(x)$ and \bar{x} are related by the law of large numbers which states that if $E(x)$ is finite, \bar{x} tends to limit $E(x)$ as N approaches infinity (X-5 Monte Carlo team., 2003).

3.6.2 Relative Error

The estimated relative error is defined as the ratio of the estimated standard deviation of the sample mean $S_{\bar{x}}$ and the sample mean \bar{x}

$$R \equiv \frac{S_{\bar{x}}}{\bar{x}} \quad (3.19)$$

The relative error for large numbers is expressed as follows

$$R = \left[\frac{1}{N} \left(\frac{\overline{x^2}}{\bar{x}^2} - 1 \right) \right]^{\frac{1}{2}} = \left[\frac{\sum_{i=1}^N x_i^2}{\left(\sum_{i=1}^N x_i \right)^2} - \frac{1}{N} \right]^{\frac{1}{2}} \quad (3.20)$$

A detailed derivation of the above equation can be found in (X-5 Monte Carlo team., 2003).

3.6.3 Variance of Variance

Variance is a measure of population of points. It is the measure of the spread of these points and it is given by

$$\sigma^2 = \int (x - E(x))^2 f(x) dx = E(x^2) - (E(x))^2 \quad (3.21)$$

The standard deviation in Monte Carlo is defined as the square root of variance σ for large numbers

$$S^2 = \frac{\sum_{i=1}^N (x_i - \bar{x})^2}{N-1} \approx \overline{x^2} - \bar{x}^2 \quad (3.22)$$

And the estimated variance of the mean \bar{x} is given by

$$S_N^2 = \frac{S^2}{N} \quad (3.23)$$

The variance of variance VOV is given by

$$VOV = \frac{S^2(S_x^2)}{S_x^4} \quad (3.24)$$

Where

S_x^2 is the estimated variance of the \bar{x} and $S^2(S_x^2)$ is the estimated variance in (S_x^2) .

Variance of variance gives a measure of the statistical uncertainty in the estimated error R, and hence the importance to Monte Carlo calculations and tally assessment.

3.6.4 History Score Probability Density

The history score of a tally bin can be seen as being sampled from an unknown history score PDF $f(x)$, where x is a random variable from one complete particle history of a tally bin. The quantity $f(x)$ is the probability of scoring between x and $x + dx$ for the tally bin. Each tally bin has its own $f(x)$

the general form of $f(x)$ is given as:

$$f(x)dx = f_c(x) + \sum_{i=1}^n p_i \delta(x - x_i) \quad (3.27)$$

Where $f_c(x)$ is the continuous and non-zero part and $\sum_{i=1}^n p_i \delta(x - x_i)$ represents n different discrete components occurring at x_i with a probability of p_i . The $f(x)$ function may be composed of either or both parts of the distribution.

The PDF is defined as

$$\int_{-\infty}^{\infty} f(x) dx \equiv 1 \quad (3.28)$$

Using the central limit theorem; when “complete” sampling has occurred the largest values of the sample x 's (i.e. histories) should have reached the upper bound or decrease faster than $\frac{1}{x^3}$ (X-5 Monte Carlo team., 2003).

After looking at the MCNP theory, the next chapter covers how the input file for all the three reactors were designed and simulated. Design parameters and physical geometry information of each reactor design are explicitly described in the next chapter.



CHAPTER FOUR

4.0 METHODOLOGY

4.1 Introduction

For every reactor type, neutronics analysis can be performed with codes based on both deterministic and Monte Carlo approaches as described in Chapter 3. The multipurpose Monte Carlo particle transport codes generally have the capability to model and treat different complicated geometries in 3-D and also simulate the transport behaviour of different particles and nuclear interaction processes. Good and accurate modelling of the different zones and diverse geometries of a reactor is important for achieving good neutronics, particle transport simulation, and physics analysis. For this reason, the versatile and widely utilized MCNP code particle transport code was employed to develop a 3-D Monte Carlo model for particle transport simulation and neutronics safety analysis for the reactors under consideration (Motwendi, 2014).

In this chapter, the 3-D Monte Carlo developed for the reactors using the MCNP5 transport code and upon which this work is derived is described. The methodology adopted in modelling and neutronic simulations relevant to this study is also presented. A completed input model would comprise a completed neutronic-thermal hydraulic calculation.

However, it should be noted that, in this study, only neutronic calculations were performed. Since the thermal hydraulic calculations were not performed, the temperatures of all the material at normal operation conditions were taken to be 300 °C and the density of the moderator was taken to be 0.98 gcm⁻³.

4.2 MCNP5

As explained in Chapter 3, the MCNP is a general-purpose Monte Carlo N-particle code that is used to simulate transport of various particle types (such as neutron, photon, electron or coupled neutron/photon/electron) while treating an arbitrary three-dimensional configuration of material in a geometry of a system, taking into account point wise continuous energy cross section libraries that represent nuclear reactions in the 10^{-11} to 20 MeV energy range.

MCNP5 is based on Monte Carlo methodology that simulates particle events and tracking of these events, with all the physics contained in the probability distribution functions. The MCNP5 permits a very general, detailed representation of 3-D geometry. Volumes in space called cells are defined with respect to their bounding surfaces. Nuclear data for fissile and non-fissile isotopes associated with materials (fuel meat, clad coolant and moderator) of the physical model was chosen from ENDF/B-VII nuclear data libraries. The special $S(\alpha,\beta)$ scattering feature was applied in the nuclear model to treat thermal scattering in hydrogen in light water for the water regions of the reactor models. The results specified to be calculated by the user are made available by the use of tallies (MCNP5, 2003).

For this study MCNP, Version 5, release 1.40 and with ENDF/B VII release 8 cross-section data were used.

4.2.1 MCNP5 Input File Description

In order to build a representative MCNP model of the reactor fuel assemblies an input file has to be developed, where the 3-D geometry is modelled and surfaces making up the geometry are described together with the material contained in the geometry (X-5 Monte Carlo team., 2003).

The MCNP input file is divided into three basic sections (excluding the message block).

Section 1	Title Cards Cell Cards
Section 2	Blank line delimiter Surface Cards
Section 3	Blank line delimiter Data Cards Blank line delimiter Anything else(Optional)

Table 4.1: Sections of MCNP Input file

I. Section 1/Title card

The first card after the optional entry in an MCNP input file is the title card where the user can specify the title of the input file.

II. Section1/Cell cards

Cell cards contain information about material (e.g. number/mass density) contained in a cell and a 3D (i, j, k) description of the geometry volume containing the material. The general format for cell cards specification is as follows “j m d geo parmet”.

Where j denotes the cell number, ‘j’ should be a positive integer of value.

The entry ‘m’ denotes the material number that specifies the material contained in a cell and the entry should also be a positive integer of value 99999. The entry “d” denotes either the mass density or number density of the material contained in a cell. A positive entry for the density is interpreted as the atomic density in units of 10²⁴ atoms per barn-centimetres, while a negative entry is interpreted as a mass density in units of grams

per cubic centimetres. The entry “geo” denotes geometry specification; it uses Boolean operators together with allocated surface numbers to describe how surfaces bind regions of space to form a cell. The “parmet” entry may be used to denote cell parameters on the cell card line rather than in the data card section. For example the cell card importance “imp:n” which specifies the relative cell importance for neutrons.

III. Section2/Surface cards

Surface cards contain information about the surface making up the geometry of the problem of interest. A surface is defined in Cartesian co-ordinates as $f(x, y, z)$. The MCNP input line defining a cylindrical surface is represented as CZ or (cz, MCNP is not case sensitive).

The direction of the surface is defined mathematically as $f(x, y, z) > 0$, which represents the positive side of the surface and $f(x, y, z) < 0$, represents the negative side of the surface. For example a region inside a cylindrical surface is negative with respect to the surface and a region outside the cylinder is positive with respect to the surface.

IV. Section3/Data cards

Data cards contain information about the mode of calculation of interest, material specification, source specification and tally types.

The specification of materials filling the cells in an MCNP model involves the following

- a) Assigning a material number to each cell.
- b) Defining the material isotopic composition.
- c) Cross section compilations to be used.

The isotope number ZAID (Z A IDentification) consists of six digits ZZZAAA where ZZZ is the atomic number Z and AAA is the atomic mass number A.

The criticality source type in MCNP is specified by the SDEF and or KCODE command. For this study a general criticality source was used in the KCODE command. The KCODE command has several variables or parameters that are used to define the source characteristics. The KSRC is also used to define source position in Cartesian coordinates.

The tally cards are used to specify the type of tally the user is interested in investigating. Fission energy deposition averaged over a cell, neutron flux averaged over a cell, etc. Tallies are defined by a tally type and particles type. Tallies are numbered as 1, 2, 4, 5, 6, 7, 8, or increments of 10 thereof and are given particle designator: P, :N, or :E. Only tally type F4 is investigated in this study and therefore only F4 tally described.

4.3 MCNP5 Model of the Reactors

In order to build a representative MCNP model of the respective reactors, all the fuel assembly design details discussed in section 2.2 were used. The MCNP models of the reactors described below cover all important details of their fuel assembly designs. The model was built as precisely to the design specifications as possible, with inherent MCNP geometric modelling inadequacies introduced in the process. The model description and assumptions are discussed in the ensuing sections.

PARAMETERS	DIMENSIONS (mm)		
	EPR	HPR	VVER
Fuel pin diameter	9.5	9.5	9.1
Cladding thickness	1.14	1.14	0.69
Gap	0.16	0.168	0.88
Fuel part diameter	8.2	8.192	7.53
Step between rods	12.6	12.6	12.75
Length of active height	4199.99	3658	3530
Number of fuel rods	265	265	312

Table 4.2 Fuel Assemblies Design Specifications

The following assumptions were made in developing the model:

- Steady state
- No temperature feedback
- No burn up/fresh fuel core
- Beginning of life
- No xenon
- Boron concentration 1383 ppm
- The assembly side boundaries are periodic for infinite assembly models

The EPR and HPR have very similar geometry and their MCNP5 input model is discussed in the next section.

4.3.1 Model of the HPR and EPR

The EPR and HPR both have a square lattice and 265 fuel pins within the fuel assembly except for difference of small millimetres in the fuel meat diameters. Using the Lattice and Fill cards of the MCNP5, the input file of the HPR fuel assembly is designed with a square lattice containing 265 fuel pins. The fuel pins have an enrichment of 1.8% (minimum enrichment for a fresh core) and are immersed in the moderator/coolant (light water) with a density of 0.98 g/cc.

In designing the EPR input deck, just as was done for the HPR, the Lattice and Fill cards of the MCNP5 were used to model the square lattice containing the 265 fuel pins. The fuel pins are surrounded by the light water moderator also with a density of 0.98 g/cc. The EPR fuel pins are modelled with an enrichment of 1.4% (minimum enrichment for a fresh core).

The design parameters of the HPR and EPR model used in designing the MCNP input file are presented in Table 4.2 above. The MCNP geometry plot card is used to view the geometry modelled for the HPR and EPR and the pictorial view presented in the Figures below.



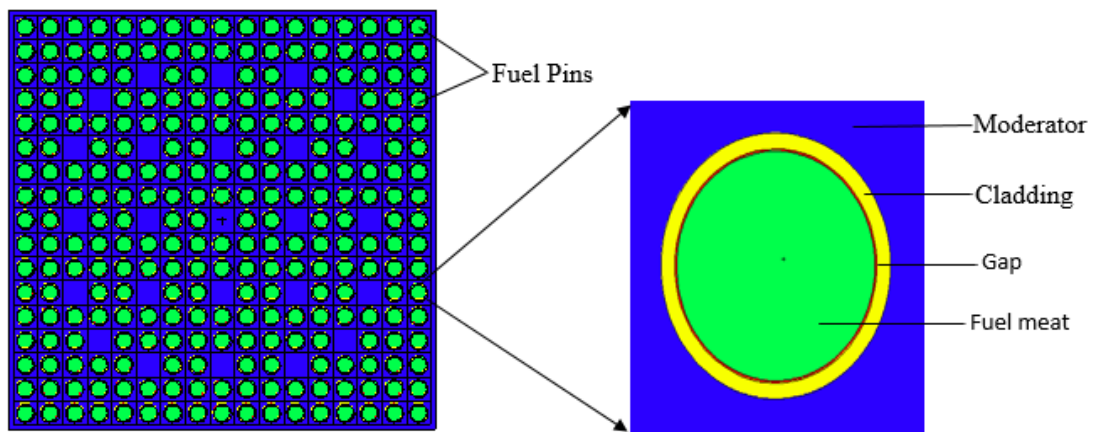


Figure 4.3 MCNP5 Plot of Transverse Section EPR and HPR Fuel Assemblies

4.3.2 Model of the VVER

Unlike the EPR and HPR, the VVER has a significantly different geometry. The 312 fuel pins of the VVER fuel assembly are arranged in a hexagonal lattice. To design the VVER input deck, the Lattice and Fill cards of the MCNP5 was used to model the square lattice containing the 312 fuel pins but this time, $lat=2$ was used to specify the triangular lattice instead of $lat=1$ that was used to specify the square lattice for both the EPR and HPR fuel assemblies. Like the other two reactor discussed earlier, the minimum enrichment of a fresh VVER core which is 1.6% is used for the modelling. The fuel pins are surrounded by the light water moderator/coolant with a density of 0.98 g/cc.

The design parameters are given in Table 4.2. The Figure 4.4 below shows the MCNP5 plot of the transverse section of the VVER fuel assembly.

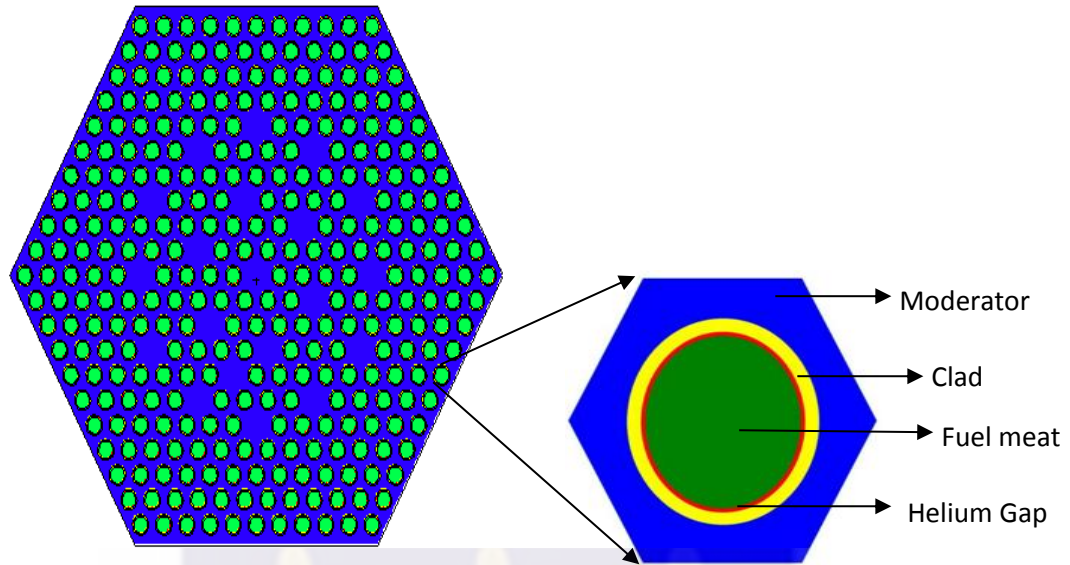
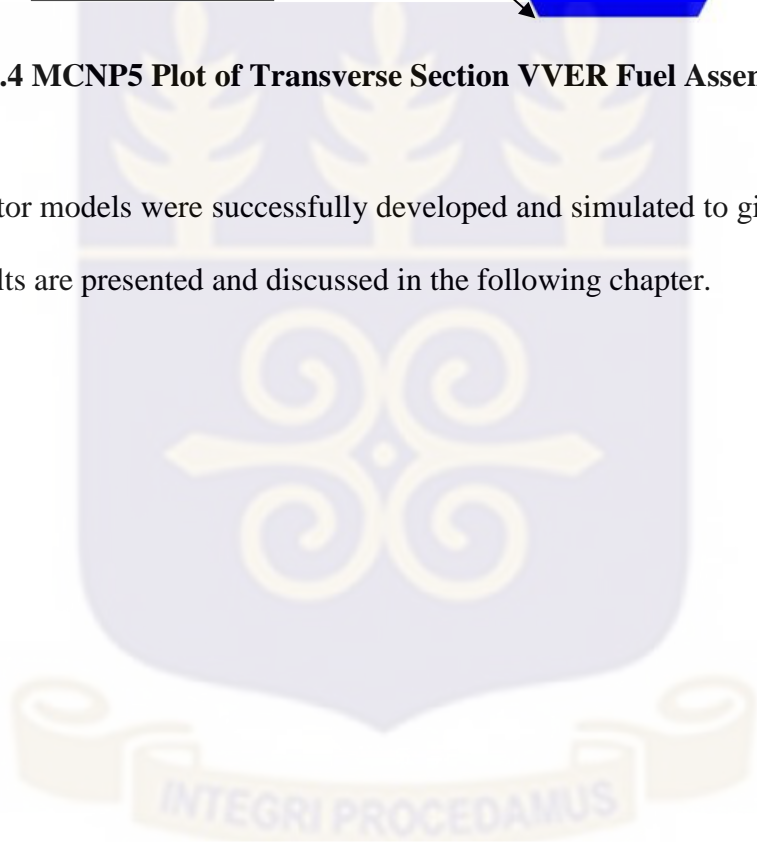


Figure 4.4 MCNP5 Plot of Transverse Section VVER Fuel Assembly

The reactor models were successfully developed and simulated to give desired results.

The results are presented and discussed in the following chapter.



CHAPTER FIVE

5.0 RESULTS AND DISCUSSION

5.1 Introduction

The engineering design of nuclear reactors is significantly influenced by the properties of the materials of the various components of the reactor. The reactor characteristics limits the choice of nuclear fuel, the fuel enrichment, the type of moderator and coolant to be utilized, the operating temperatures and pressures in the core.

In nuclear power reactors, changes to these parameters and operating conditions mentioned earlier influences the reactivity of the reactor in different ways. The total reactivity coefficients consist of reactivity changes due to fuel temperature changes, moderator temperature changes and changes of void content. For a pressurized water reactor working in steady state, the changes in reactivity due to temperature changes is the most significant. The changes in reactivity due to void content becomes very important when simulating a LOCA situation.

5.2 Moderator Void Reactivity

As already stated in section 5.1 of this chapter, the multiplication factor of a reactor depends on the moderator void content of the reactivity for safe operation. As a result, a change in the moderator void content leads to a change in multiplication factor (k) and alters the reactivity of the system. The void coefficient of reactivity is therefore defined as the rate of change in the reactivity of a water moderated reactor resulting from any modification of the moderator/coolant as the power level and temperature changes.

In a PWR, almost all the neutron moderation take place in the light water moderator resulting in the desired thermal flux peaks in the reactor. This makes the multiplication

factor very sensitive to density and temperature changes of the materials making up the reactor core. A negative moderator void coefficient is more desirable. This is because, the PWRs like all other thermal reactor designs require that, the fast fission neutrons are thermalized in order to interact with the fissile isotopes in the fuel to sustain the fission chain reaction. The moderating of neutrons is much more effective if the moderator water is denser (more collisions will occur). If the quantity of void increases, the moderator expands creating more gaps between the water molecules and hence reducing the probability of thermalization of the fast fission neutrons. This in effect reduces the number of thermalized neutrons that can cause fission thereby reducing the reactivity in the core. This is an important safety feature in Pressurized Water Reactors.

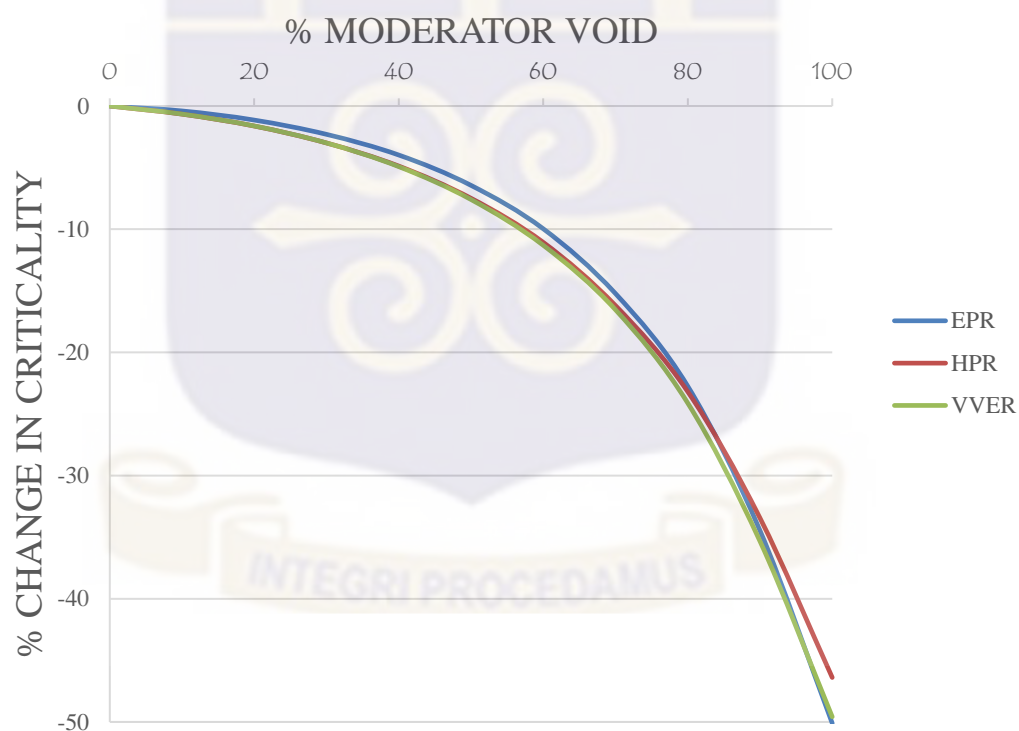


Figure 5.1 Moderator Void for the Three Assemblies

All three reactor assemblies simulated in the study are composed of UOX fuel and have desirable moderator void reactivity at all stages of moderator void fraction (see Figure

5.1). The UOX fuel is designed to operate in the thermal spectrum and it goes subcritical when there is loss of thermal neutrons. The loss of thermal neutrons is associated with loss of light elements in the core as a result of loss of coolant hence the loss of thermal neutrons to fission with the fissile isotopes to sustain the chain reaction.

The neutron behaviour at varied void content is clearly shown in Figures 5.2, 5.3 and 5.4 below for each reactor assembly.

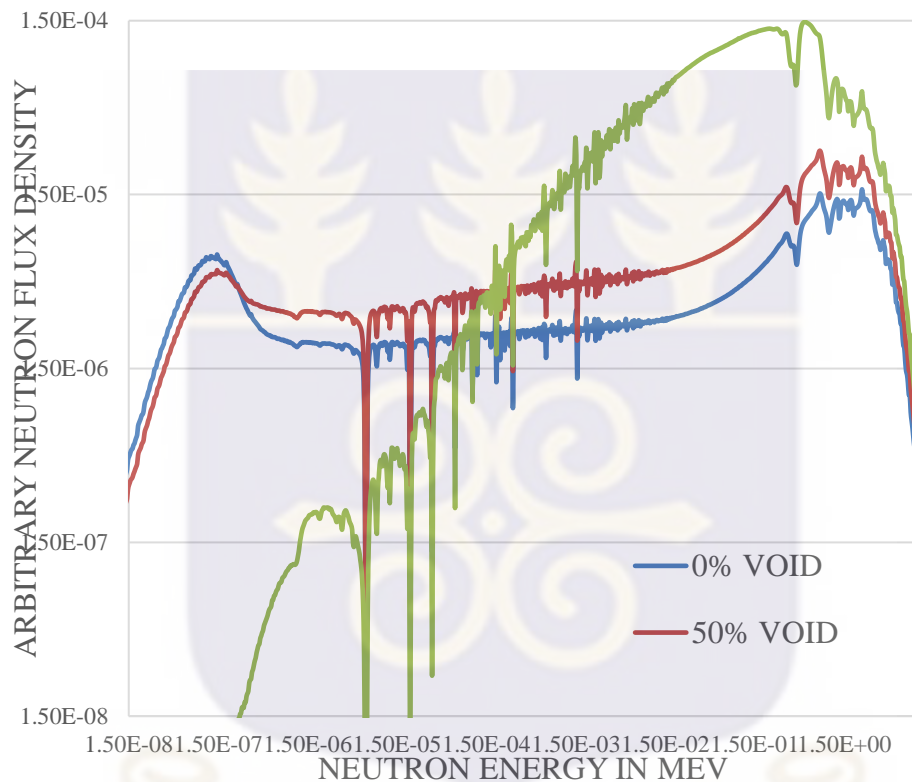


Figure 5.2 Neutron Spectra of different percentage of Loss of Coolant for the EPR Assembly

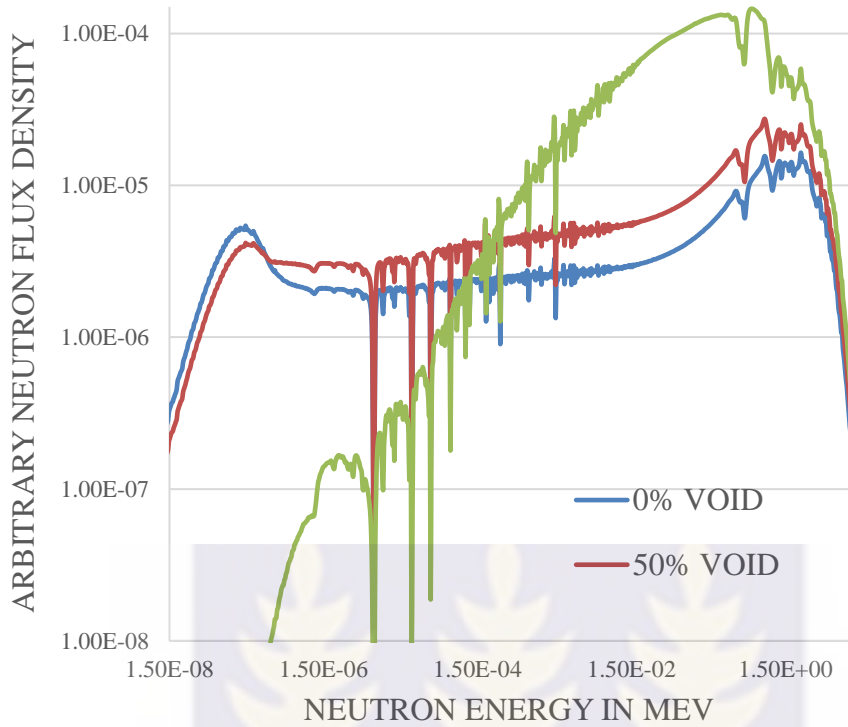


Figure 5.3 Neutron Spectra of different percentage of Loss of Coolant for the HPR Assembly

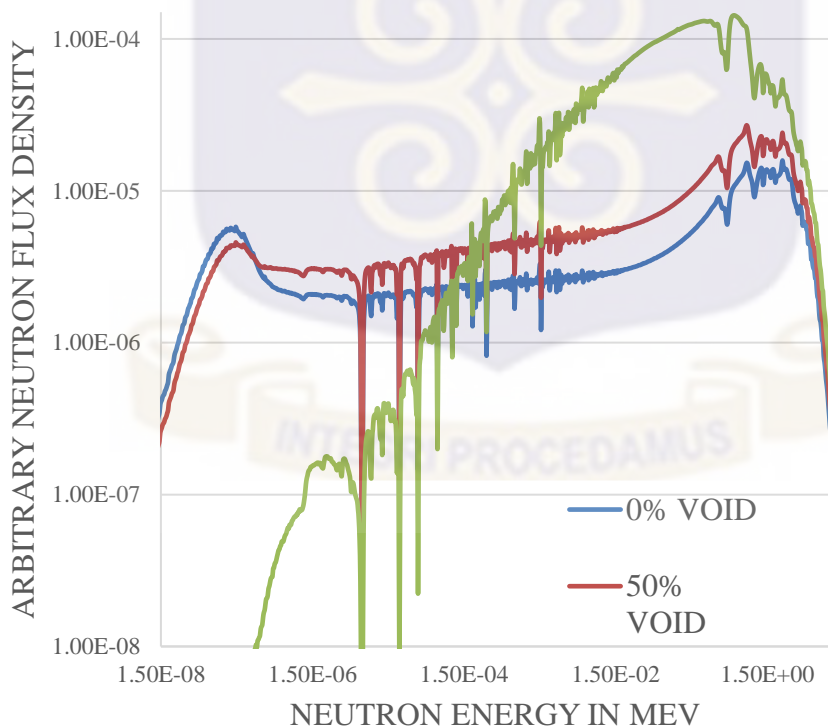


Figure 5.4 Neutron Spectra of different percentage of Loss of Coolant for the VVER Assembly

5.2.1 Moderator Void Coefficient of Reactivity

The amount of reactivity (ρ) in a reactor core determines the neutron population and the reactor power at any given time. To quantify the effect of the variation in void content on the reactivity of the core, the moderator void coefficient is used. The moderator void coefficient of reactivity which is the amount of change in the reactivity with a given change in moderator void content is mathematically expressed as;

$$\alpha_x = \frac{1}{k_\infty} \frac{dk_\infty}{dx} \quad (5.1)$$

Or;

$$a_x = \frac{\Delta\rho}{\Delta x} \quad (5.2)$$

$$\rho = \frac{k_\infty - k_0}{k_\infty} \quad (5.3)$$

Where a_x is the reactivity coefficient of the parameter x , k_∞ is the infinite multiplication factor, ρ is the reactivity. In this analysis, the parameter x represents the coolant density (moderator void).

Equations 5.2 and 5.3 were used in the analysis of the coefficients because, the results obtained from the simulation were given in k_∞ which is inserted in Equation 5.2 to calculate ρ . The resulting ρ is then inserted into Equation 5.3 to calculate the coefficients (a_x). It must be noted that both mathematical definitions give similar results for analysis of situations not far from the criticality. To calculate the void coefficient of reactivity, all other parameters are kept constant. The results from the calculations are given in the Table 5.1.

From the results in Table 5.1, the following deductions can be made;

- Reactivity changes due to variation of coolant density (void content) by 10% of the normal density for all the three different reactor assemblies.
- All the reactors have negative moderator void coefficients of reactivity at all stages of increase in the reactor void (decrease in coolant density). This means that all the reactors respond to increase in void fraction by going subcritical and eventually shutdown if the loss of coolant is not mitigated. This is a very important safety feature. Because it is important that more heat is not generated during coolant loss.
- The larger the absolute value of the reactivity coefficient, the further the reactor is from criticality. The VVER assembly has the largest absolute value for the coefficients of reactivity from 0% to 80% void fraction of all the reactor assemblies. This makes the VVER the safest in the case of coolant loss because the large negative reactivity makes it subcritical and shutdown quicker compared to the other assemblies.

Void Range %	Coefficient of Reactivity		
	EPR	HPR	VVER
0-10	-0.04073501	-0.067942041	-0.067222923
10-20	-0.07700235	-0.100794371	-0.100864867
20-30	-0.12252846	-0.146902789	-0.147341661
30-40	-0.18242773	-0.207326331	-0.212568141
40-50	-0.27973985	-0.303010506	-0.310190817
50-60	-0.42717926	-0.444101632	-0.462475996
60-70	-0.70283506	-0.702349479	-0.721537363
70-80	-1.17127094	-1.107637638	-1.219889907
80-90	-2.36255624	-2.047544738	-2.33161644
90-100	-5.42159943	-4.114301779	-4.958304521

Table 5.1 Moderator Void Coefficient of Reactivity at Different Void Fraction

5.2.2 Neutron Spectra of Different Reactors with Same Void Content

Fission neutrons are born fast with average energy of 2MeV. Neutrons with energy greater than 0.1MeV are considered to be in the fast region of the neutron spectrum. In thermal reactors, the flux in the intermediate region (1eV to 0.1MeV) has approximately $1/E$ dependence. This $1/E$ dependence is due to the slowing down process, where elastic collision with moderator material remove constant fraction of neutron energy per collision (on the average) independent of energy. This makes the neutrons tend to “pile up” at lower energies, that a significant neutron flux density at the neutron energies corresponding to the thermal neutron energy region on the spectrum.

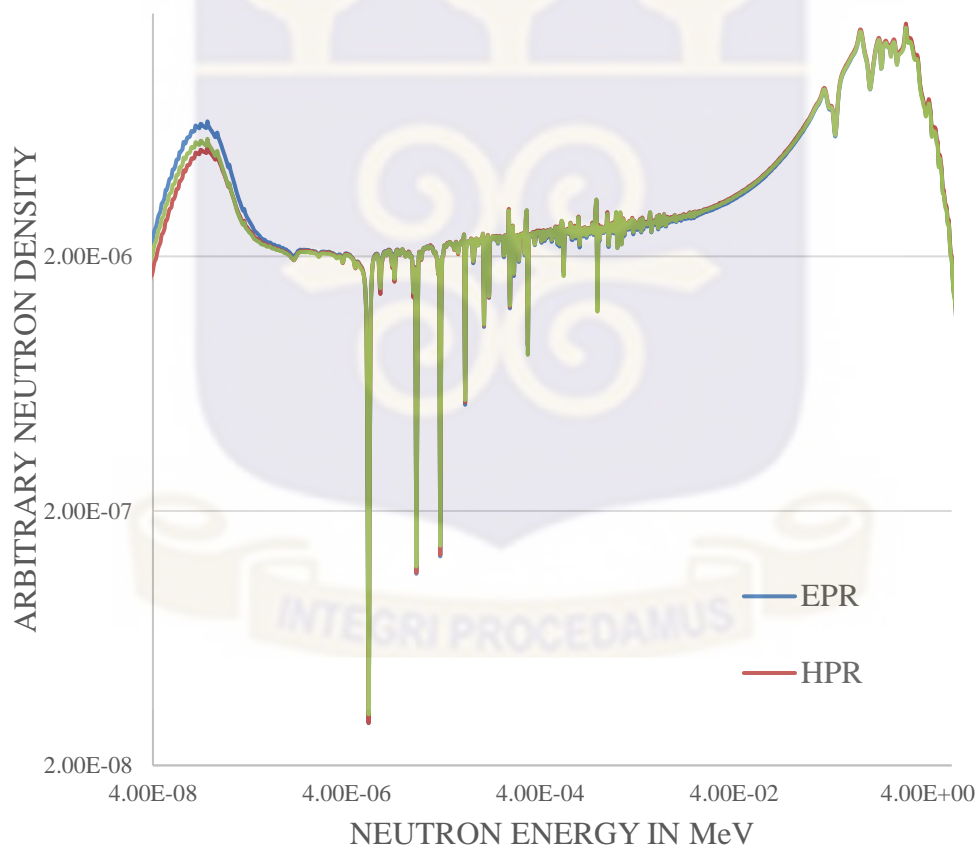


Figure 5.5 Neutron Spectra for EPR, HPR and VVER at Normal Operating Void

From the Figure 5.5, the EPR, HPR and VVER depict a typical neutron spectrum of thermal reactors. At normal operating conditions, there is enough light elements from

the water moderator for effective slowing down of fast fission neutrons hence the similarity of the three spectra. However, neutron thermalisation in the EPR is more effective than in the other reactors, the reason for the highest amplitude of the curve in the thermal region of the spectrum representing the neutron behavior in the EPR.

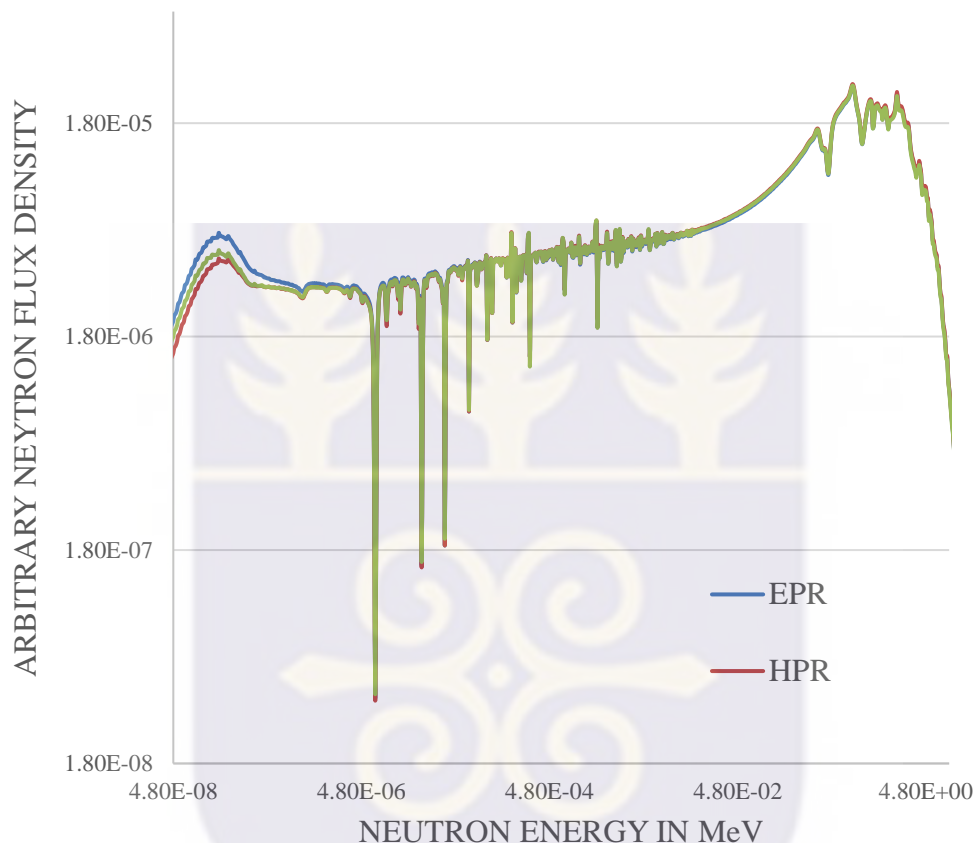


Figure 5.6 Neutron Spectra of EPR, HPR and VVER at 50% Void

If the moderator is reduced to half of the required volume, the moderator water expands and creates a large amount of void within the reactor. This significantly reduces the amount of light hydrogen atoms in the core responsible for slowing down the fast fission neutrons. In effect, the slowing down process is largely reduced and the neutron flux density in the thermal region is significantly reduced.

The Figure 5.6, shows neutron density in the thermal region of the spectra, this is because neutron moderation still occurs at the 50% void. Comparing the neutron spectra

in Figure 5.6 to Figure 5.5, the neutron flux density in the thermal region of the Figure 5.6 is less due to loss of coolant in all three reactor assemblies.

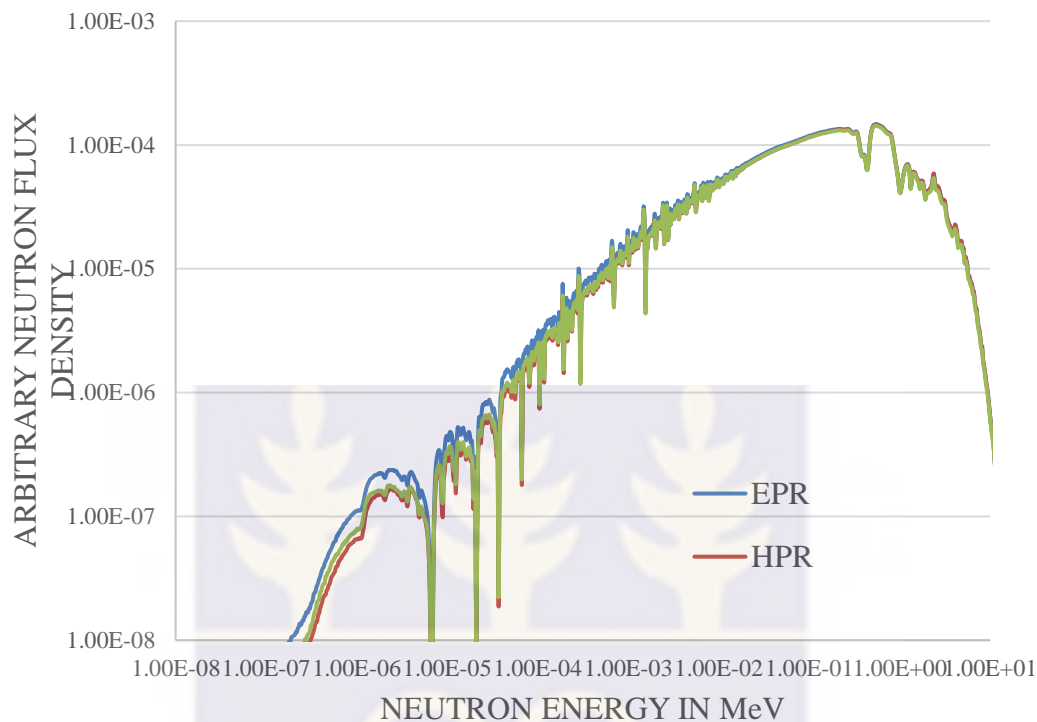


Figure 5.7 Neutron Spectra of EPR, HPR and VVER at almost 100% Void

The shape of the spectra in Figure 5.7 is attributed to the absence of moderation of fast fission neutrons. In the figure, not even one of the reactor assemblies shows neutron flux density in the thermal neutron energy region of the spectra, although there is neutron flux density in the epithermal region of the spectrum due to interactions with the core structural materials. For a thermal reactor, this situation can lead to any of these two cases;

1. The absence of thermal neutrons to fission with the fissile U-235 in the fuel causes the reactor to go subcritical and eventually shutdown.
2. The U-238 in the fuel transmutes to Pu-239 by neutron absorption followed by beta decay. The resulting Pu-239 fissions by interacting with the high energy neutrons to sustain the fission chain reaction in the core.

For these thermal reactors under such loss of coolant conditions, the case 1 is desirable.

Case 2 is observed in breeder reactors and very unlikely in thermal reactor systems.

From the Section 5.2.1, the reactivity changes at such severe loss of coolant situations is very large and negative and can only lead to reactor shutdown.

5.3 Moderator Temperature Reactivity

The influence of temperature on the neutron transport is caused by the thermal movement of nuclei influencing the scattering of thermal neutrons and the Doppler broadening of resonances and by the thermal expansion different materials within the core.

Reactivity changes associated with a degree change in the moderator temperature is referred to as the moderator temperature coefficient of reactivity. Globally, the temperature coefficients of the fuel assemblies under consideration are negative with increasing temperature from 0% to 100% of the nominal operating temperature of 575K for the moderator. A negative moderator temperature coefficient is desirable because of its self-regulating effect (Sogbadji, 2012).

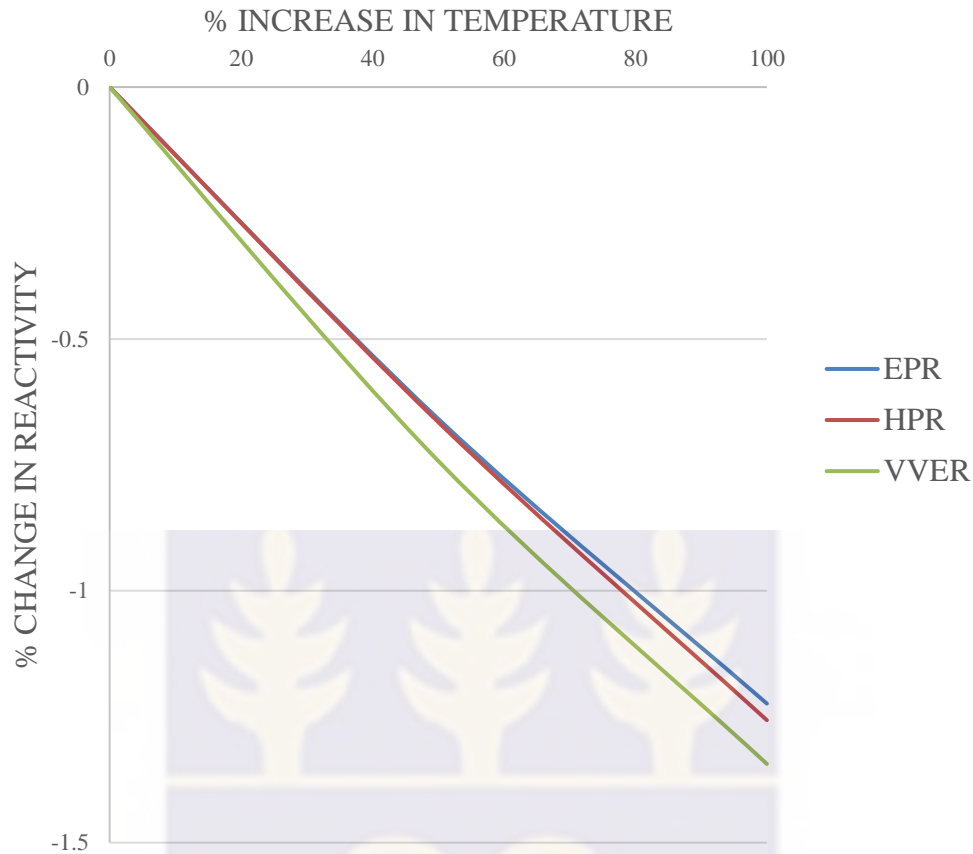


Figure 5.8 Moderator Temperature Coefficient of the Three Reactor Assemblies

The moderator temperature coefficient of all the reactor assemblies considered are desirable since the reactivity decreases with increasing moderator temperature as shown in Figure 5.8. An increase in the moderator temperature makes the core under moderated due to the increase in energy of the lighter nuclides that can cause moderation. An under moderated reactor gives a negative moderator temperature coefficient while an over moderated reactor will give a positive moderator temperature coefficient.

Comparably, the VVER assembly shows the best moderator temperature coefficient of all the reactor assemblies considered. During moderator void or loss of coolant in the core, the moderator or coolant temperature tend to increase as well. The negative

reactivity feedback of the moderator temperature coefficient tends to compliment the negative feedback of the Coolant Void Reactivity in the previous section.

5.4 Doppler Effect of U-238 on Reactivity

In a typical low enriched light water reactor, as indicated earlier, the fuel temperature coefficient of reactivity is negative, this is due to the Doppler effect of the large percentage of U-238 in the fuel also known as the Doppler broadening. The phenomenon of the Doppler broadening is as a result of the apparent broadening and shortening of resonance peaks due to thermal motion of nuclei. The Doppler reactivity coefficient is another name for the fuel temperature coefficient of reactivity.

Stationary nuclei absorb only neutrons of specific energy, say E_0 . If the nucleus is moving away from the neutron, the velocity (and energy) of the neutron must be greater than E_0 to undergo resonance absorption. Likewise, if the nucleus is moving toward the neutron, the neutron needs less energy than E_0 to be absorbed. Raising the temperature causes the nuclei to vibrate more rapidly within their lattice structures, effectively broadening the energy range of neutrons that may be resonantly absorbed in the fuel. Two nuclides present in large amounts in the fuel of some reactors with large resonant peaks that dominate the Doppler Effect are uranium-238 and plutonium-240 (Sogbadji, 2012).

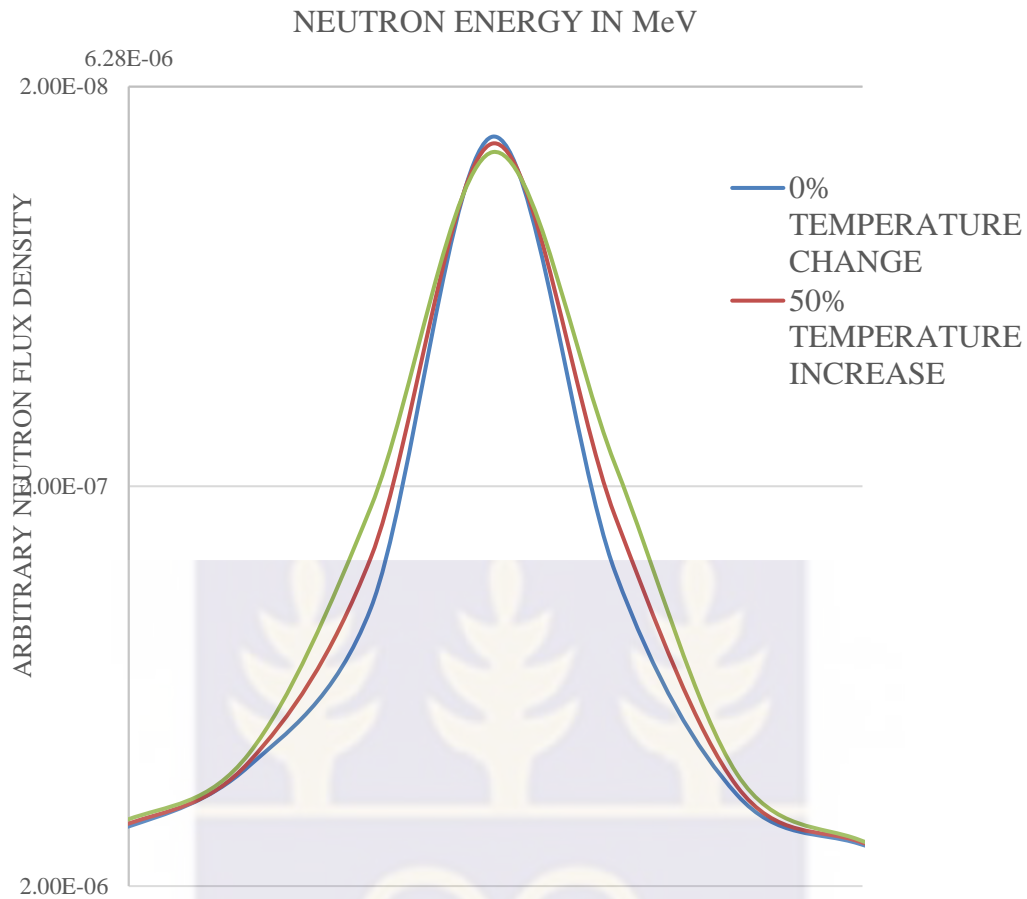


Figure 5.9 Doppler Broadening Effect in EPR Assembly at 6.74eV Resonance Peak

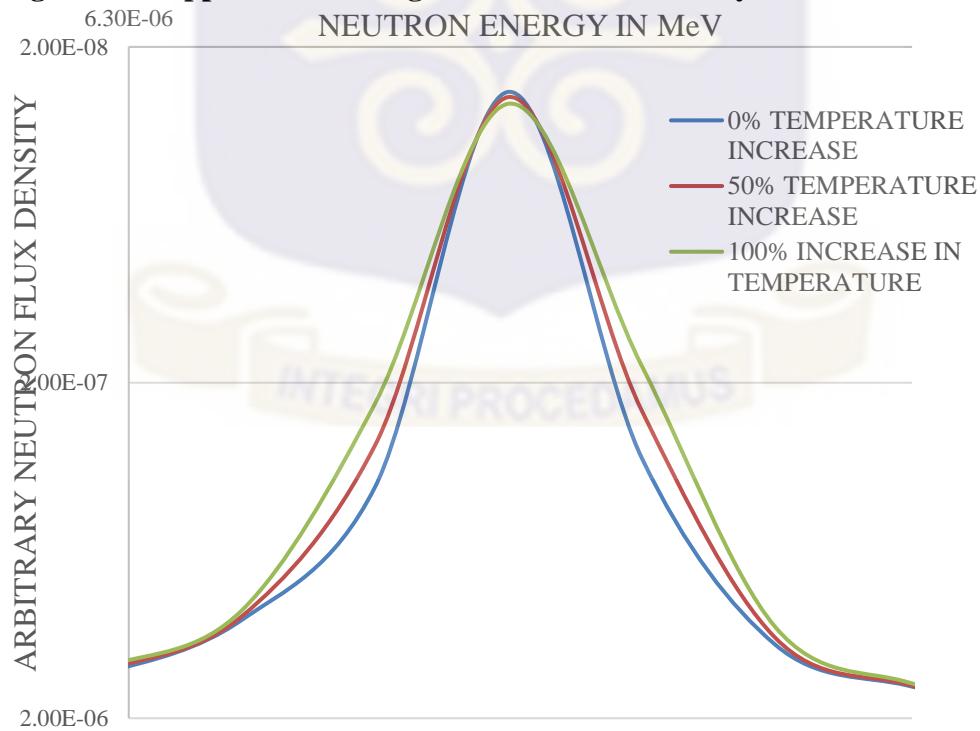


Figure 5.10 Doppler Broadening Effect in HPR Assembly at 6.74eV Resonance Peak

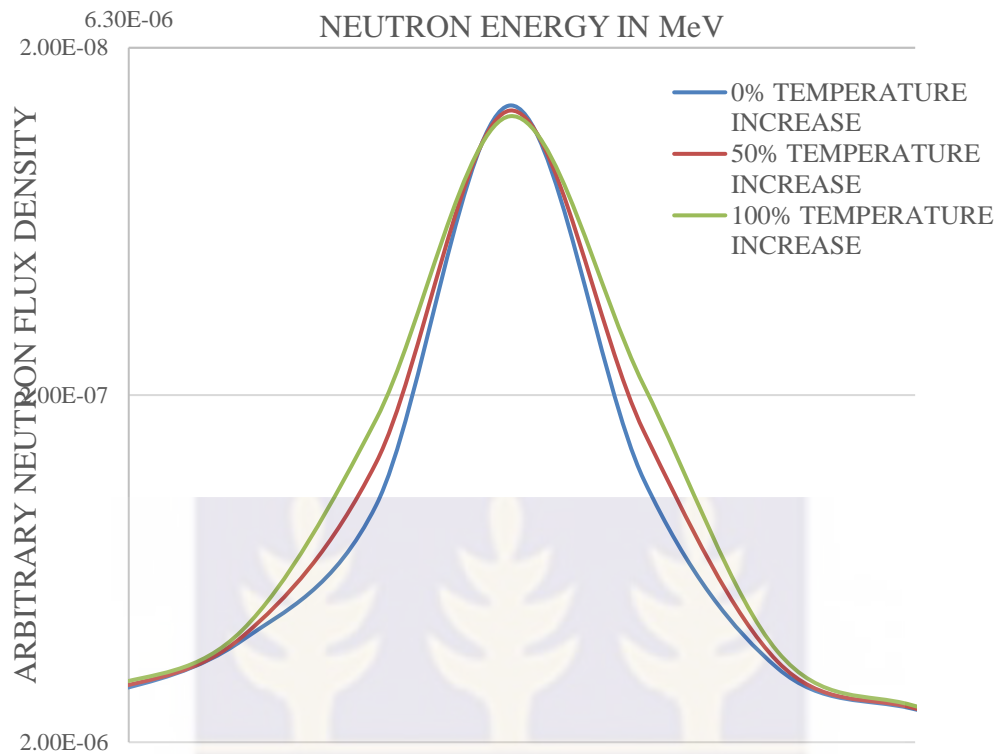


Figure 5.11 Doppler Broadening Effect in VVER Assembly at 6.74eV Resonance Peak

The Doppler broadening effect is observed in all low enriched UO_2 fuel. As shown in Figures 5.9, 5.10 and 5.11, the peak width in the resonance region of the spectrum increases with increasing temperature. In the same figures, the peak heights reduce with increasing temperature. This does not affect the neutron absorption probability in the resonance region because the broadening of the peak width increases the range of neutron energy that can be absorbed to compensate for the decreased absorption cross section as a result of the reduction in the pulse height.. Since there is over 80% of U-238 in all the fuel assemblies simulated in this work, this effect is replicated in all the three reactor assemblies.

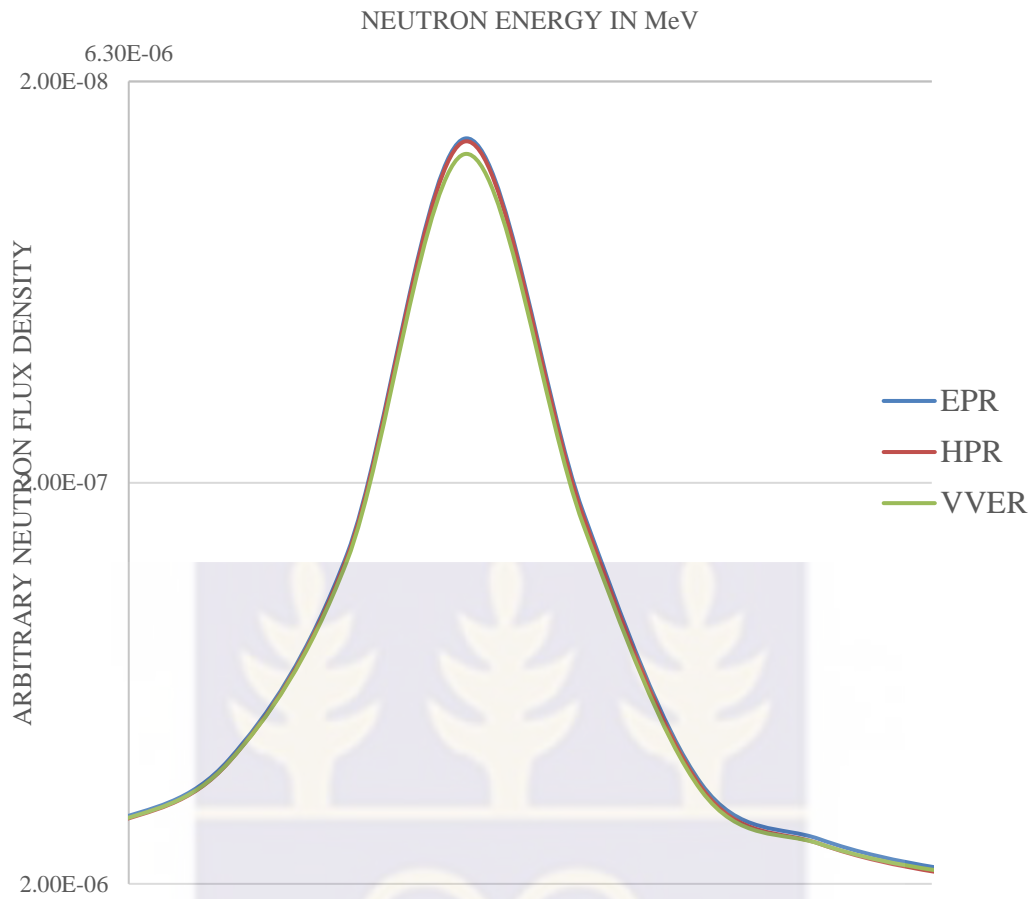


Figure 5.12 Doppler Effect of the Three Reactors at 50% Increase in Temperature at 6.74eV Resonance Peak



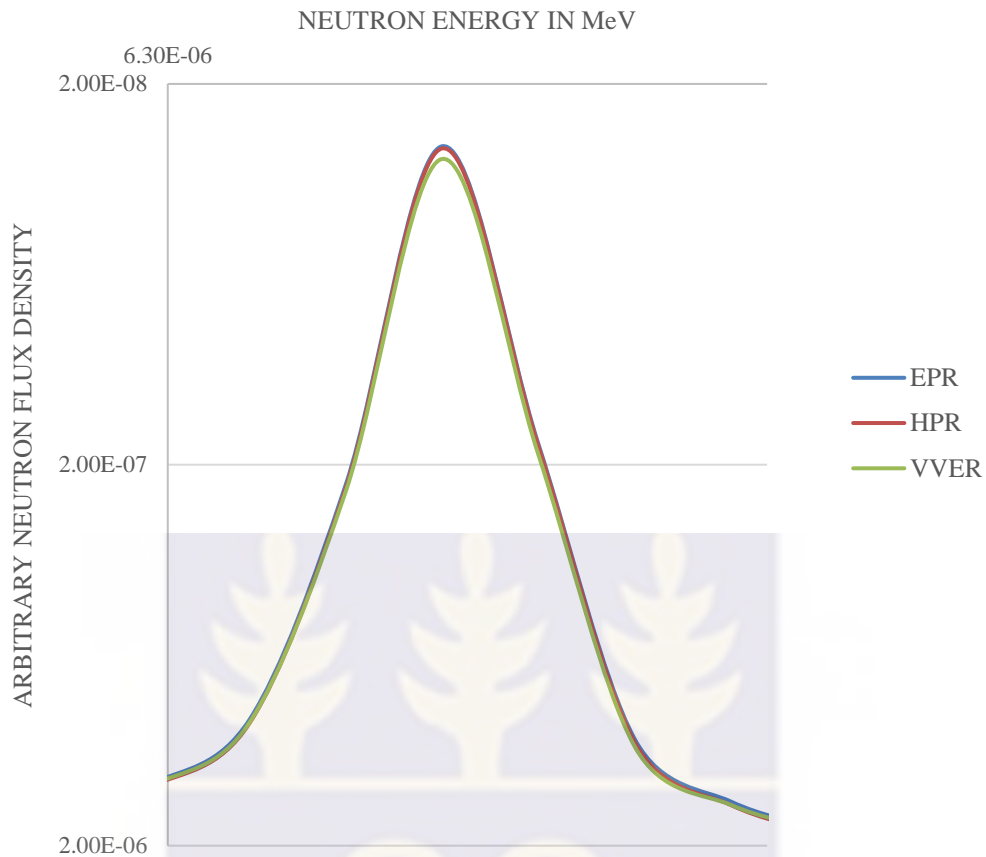


Figure 5.13 Doppler Effect of the Three Reactors at 50% Increase in Temperature at 6.74eV Resonance Peak

In Figures 5.12 and 5.13, the Doppler Effect at 50% and 100% increment in temperature is compared for the different reactor assemblies. The figures presented show similar pulse width for all the reactors. Although all technologies showed Doppler broadening with increasing temperature, the EPR had the highest absorption cross section, showing a higher safety margin.

The next chapter focuses on the conclusions drawn from the analysis of the results in this chapter. Appropriate recommendations based on the study is given in the next chapter.

CHAPTER SIX

6.0 Conclusion and Recommendation

6.1 Conclusion and Recommendations

The input deck of the MCNP model for the three nuclear power reactors; EPR, HPR and VVER were successfully developed to represent the full core. The criticality was determined for each reactor at normal operating conditions and the associated neutron spectra of all the reactors at the normal operating conditions. Also, further simulations were run to determine how each reactor responds to changes to the operating conditions or accident scenarios.

All three reactors are critical and give a typical neutron spectra synonymous to all thermal nuclear reactors at normal operating conditions. Also, all the reactors showed inherent safety features with respect to void fraction by adding significant negative reactivity to return the reactor to normal operation or eventual shutdown to mitigate loss of coolant accident. The reactors again show inherent passive safety feature with increasing temperature by adding negative reactivity to the core to restore the reactor to normal operation.

For Ghana's choice of nuclear power technology, it is recommended that, neutronic safety calculations are performed for the full core of the reactors under study using the results from this work as a benchmark. It is also recommended that, a thermal hydraulic model of the EPR, HPR and VVER should be developed and coupled to the neutronic model to form a coupled neutronic and thermal hydraulic analysis of the reactors. Burn-up analysis should be done to determine the power output and fuel utilization of the reactors over the core life. The burn-up calculations may also have a much significant

influence on the results from neutronic calculations. Possible parameters that are influenced by the burn-up include the reactor temperature reactivity (RTC) at different stages of the core life due to build-up of fission products and actinides.



7.0 References

- Aguilar, O., & Por, G. (1987). Monitoring Temperature Reactivity Coefficient by Noise Method in NPP at Full Power. *Annals of Nuclear Energy*, 1-6.
- Alhassan, E., Akaho, E., Nyarko, B., Adoo, N., & Agbodemegbe, V. Y. (2010). Analysis of Reactivity Temperature Coefficient for Light Water Moderated HEU-UA14 and LEU-UO2. *Journal of Applied Sciences Research*, 2-9.
- AREVA. (2012). *US EPR Brochure, Paris-La Defense oedex France*. Framatone ANP.
- AREVA. (2012). *US EPR Final Safety Analysis Report*. Washongton D.C: AREVA.
- Balaceanu, V., & Pavelescu, M. (2010). Neutronic Calculation System for CANDU core Based on Transport Methods. *Romanian Reports in Physics*, 1-13.
- Brettschuh, W., & Schneider, D. (2002). Modern Light Water Reactors- EPR and SWR 1000. Present status and possibilities of development and application. *IAEA; International Nuclear Information System*.
- Brown, F. B. (2005). *Fundamentals of Monte Carlo particle transport*. Los Alamos: Los Alamos National Laboratory.
- Brown, F. B. (2006). *On the use of Shannon Entropy of the Fission Distribution for Assessing Convergence of Monte Carlo Criticality Calculations*. Los Alamos: Los Alamos National Laboratory.
- CEPA, Center for Policy Analysis. (2007). Ghana: The Energy Crisis and Growth Performance of the Economy. *CEPA Issues Paper, Selected Economic Issues*, (15), 19.
- CNNC. (2015). *HPR-1000 Technology*. China National Nuclear Cooperation.
- Edenius, M. (1976). *Studies of Reactivity Temperature coefficient in Light Water Reactors*. Doktorsavhandlingar Vid Chalmers Tekniska Hogskola.
- Eshun, M. E., & Amoako-Tuffour, J. (2016). A Review of th Trends in Ghana's Power Sector. *Springer*, 2.
- Faghihi, F., Fadaei, A., & Sayareh, R. (2007). *Reactivity coefficient simulation of the Iran VVER-1000 nuclear reactor using WIMS and CITATION codes*. Prog. Nucl. Energy.
- Framatome ANP, Inc. (2005). *EPR Design Description*. Lynchburg, Virginia: Framatome ANP, Inc.
- Ghana News Agency. (2014, June 27). *nuclear-energy-necessary-for-ghanas-economic-advancement--76599*. Retrieved from <http://www.ghananewsagency.org/science>:

<http://www.ghananewsagency.org/science/nuclear-energy-necessary-for-ghanas-economic-advancement--76599>

- Glasstone, S., & Sesonske, A. (1994). *Nuclear REactor Engineering*. New York: Chapman & Hall.
- IAEA. (2013). *Nuclear power today and tomorrow*. Vienna: Austria: IAEA Bulletin.
- IAEA. (2017). *Nuclear Power Reactors in the World*. Vienna: Reference Data Series No. 2.
- Jazbec, A., Snoj, L., & Kavšek, D. (2013). Analysis of a Void Reactivity Coefficient of JSI Triga Mark II Reactor. *Nuclear Energy for New Europe*, 1-9.
- Khan, R., Villa, M., & Bock, H. (2011). Monte Carlo Modelling of Void Coefficient of Reactivity Experiment. *Vienna University of Technology*, 1-5.
- Kotlyar, D., Shaposhinik, Y., & Frindman, E. &. (2011). Coupled neutronic thermo-hydraulic analysis of a full PWR core with Monte-Carlo based BGCORE system. *ELSEVIER*(july.pp. 3778 - 3786.), 18.
- Lamarsh, J. R., & Baratta, A. J. (2012). *Introduction to Nuclear Engineering* (3rd ed.). New Jersey: Prentice Hall.
- Lamarsh, R. J. (1982). *Introduction to Nuclear Engineering*. New York: Addison-Wesley Publishing Company.
- Larmash, J. R. (1982). *Introduction to Nuclear Reactor Theory*. New York: Addison-Wesley Publishing Company.
- Larmash, R. J. (2001). *Introduction to Nuclear Engineering*. New Jersey: Prentice Hall, Inc.
- Mahlers, Y. P. (2009). VVER-1000 neutronics calculation with ENDF/B-VII data. *Annals of Nuclear Energy*, 1-6.
- Mattes, M., & Keinert, J. (2005). Thermal Neutron Scattering Data for the Moderator Materials H₂O, D₂O and Zr_x in the ENDF-6 format and ACE library for MCNP(X) codes,. *INTERNATIONAL ATOMIC ENERGY AGENCY*.
- MCNP5, X.-5. M. (2003). *MCNP- A general Monte Carlo N-Particle Transport code* (Vol. volume I). Los Alamos: Los Alamos National Laboratory.
- Miller, W. F., & Lewis, E. E. (1993). *Computational methods of Neutron Transport*. Illinois: American Nuclear Society, INC.
- Motwendi, O. (2014). *Neutronic Simulation of a European Pressurized Reactor*. Potchefstroom: North-West University.

- Odoi, C. H., Akaho, E. H., Jonah, S. A., Abrefah, R. G., & Ibrahim, V. Y. (2014). Study of Criticality Safety and Neutronic Performance for a 348-Fuel Pin Ghana Research Reactor-1 LEU Core Using MCNP Code. *World Journal of Nuclear Science and Technology*, 1-7.
- OKB GIDROPRESS. (2011). *Status and Perspective of VVER Nuclear Power Plants*. Vienna: ROSATOM.
- Okumura, K., Oka, Y., & Ishiwatari, Y. (2014). Nuclear Reactor Design.
- Pautz, A., Hasse, U., & Zwermann, W. (2005). Fuel assembly calculations using the method of discrete ordinates. *Nuclear Science and Engineering*(149(2)), pp. 197-210.
- ROSATOM. (2011). *Nuclear Fuel for VVER Reactors*. Kharkov: ROSATOM.
- Safarzadeh, O., Saadatian-Derakhshandeh, F., & Shirani, A. (2015). Calculation of reactivity coefficient with burn-up changes for VVER-1000 reactor. *Elsevier*, 1-10.
- Sanchez, V. H., & Hering, W. &. (2002). Analysis of the OECD/NEA PWR Main steam line break (MSLB) benchmark exercise 3 with the coupled code system Relap5/PANBOX. *Framatome ANP Erlangen*.
- Schneider, D. &. (2002). Modern Light Water Reactors - EPR and SWR 1000. *Framatome ANP*, 1-11.
- Singh, P. (2015). Nuclear Energy Comarison with Alternative Energy Sources. *Stanford University*.
- Sogbadji, R. B. (2012). *Neutronic Study of th Mono-Recycling of Americium in PWR and the Core Conversion in MNSR Using the MURE Code*. Paris: Univesite de Paris Sud.
- Stacey, W. M. (2007). *Nuclear Reactor Physics*. New York: John Wiley & Sons, INC.
- Tikhonov, N. (2011). *WWER-1000 Reactor Simulator*. Milan.
- Waata, C. L. (2006). Coupled Neutronics / Thermal-Hydraulics analysis of a High-Perfomance Light-Water Reactor Fuel Assembly,. *Germany: In: FZKA 7233, Forschungszentrum Karlsruhe*.
- World Bank. (2013). <http://go.worldbank.org/8VI6E7MRU0>. Retrieved from www.worldbank.org: <http://go.worldbank.org/8VI6E7MRU0>
- X-5 Monte Carlo team. (2003). *MCNP- A general Monte Carlo N-Particle Transport code*. (Vol. Volume I). Los Alamos: Los Alamos National Laboratoroty.

Yergin, D., & Gross, S. (2012). Energy for Economic Growth; Energy Vision Update. *World Economic Forum*, 6.

Zohuri, B. (2016). *Neutronic Analysis for Nuclear Reactor Systems*. New Mexico: Springer.

